CLM-R 131

CLM-R 131

UKAEA RESEARCH GROUP

Report

THE PROPAGATION OF SMALL AMPLITUDE COHERENT ELECTRON PLASMA WAVES IN Q-MACHINE PLASMA

R N FRANKLIN
S M HAMBERGER
G LAMPIS
G J SMITH

CULHAM LABORATORY
Abingdon Berkshire
1974
Available from H. M. Stationery Office

C. 18

PRICE £1

U.D.C.
533.951.2
621.039.619 ARIADNE

CLM-R 131

THE PROPAGATION OF SMALL AMPLITUDE COHERENT ELECTRON PLASMA WAVES IN Q-MACHINE PLASMA

by

R.N. FRANKLIN
S.M. HAMBERGER
G. LAMPIS
G.J. SMITH

A B S T R A C T

This report is intended to contain the essential practical details necessary to make reliable measurements of the propagation constants of small amplitude (linear), monochromatic, electron plasma waves and show how they are used to determine with high precision the electron number density and temperature. We use data obtained in the Culham Q-machine (ARIADNE) in which an almost collisionless, thermally ionized, strongly magnetized cylindrical plasma column is produced and do not discuss the pioneering experiments by Malmberg and Wharton (1965,1966) or those by Derfler and Simonen (1966): a comprehensive review of their work has been given by Gentle (1970).

UKAEA Research Group,
Culham Laboratory,
Abingdon,
Berks.

January, 1974

SBN: 85311 020 4

CONTENTS

1. INTRODUCTION

Electron plasma waves are longitudinal waves driven by the restoring electrostatic forces which occur when a group of electrons is displaced from its equilibrium position. In infinite plasma they propagate with angular frequencies ($\omega = 2\pi f$) above, but close to, the electron plasma frequency (ω_{pe}), wavelengths ($\lambda = 2\pi/k$) greater than the Debye length (λ_D), phase velocities (v_φ) higher than the electron thermal speed (v_{Te}), and, for sufficiently small amplitudes, with an exponential attenuation which becomes appreciable only when v_φ is close to v_{Te} (i.e. for $v_\varphi \leqslant 3.5\, v_{Te}$, for which $k\lambda_D \geqslant 0.2$). This damping, which occurs in the absence of collisions, arises from the resonant interaction of the wave electric field with those electrons having the same velocity as the wave phase velocity and is usually called Landau damping.

The usual assumption, following Landau's theory (1946), is that an infinite, homogeneous, unmagnetized, warm, collisionless plasma is perturbed with wave number k at time $t = 0$ and thereafter left to oscillate with angular frequency ω, the amplitude damping as $\exp(-\gamma_L t)$. For waves propagating in warm plasma with phase velocities $\geqslant 2\, v_{Te}$ (i.e. $k\lambda_D \leqslant 0.4$) he showed that

$$\omega^2 = \omega_{pe}^2 + \frac{3k^2}{n}\int_{-\infty}^{+\infty} v^2 f_o(v)\,dv + O(k^4) + \ldots \qquad \ldots (1)$$

and

$$\gamma_L = \frac{\pi}{2}\,\omega\,\frac{\omega_{pe}^2}{k^2}\left.\frac{\partial f_o}{\partial v}\right|_{v=\frac{\omega}{k}} \qquad \ldots (2)$$

where $f_o(v)$ is the unperturbed electron velocity distribution function. For plasma with a Maxwellian electron velocity distribution these become

$$\omega^2 = \omega_{pe}^2 + \frac{3}{2}k^2 v_{Te}^2 + O(k^4) + \ldots \qquad \ldots (1a)$$

and

$$\gamma_L = \sqrt{\pi}\,\omega\left(\frac{v_\varphi}{v_{Te}}\right)^3 \exp\left[-\left(\frac{v_\varphi}{v_{Te}}\right)^2\right] \qquad \ldots (2a)$$

respectively, where $\omega_{pe}^2 = 4\pi\, ne^2/m$, $v_{Te}^2 = 2KT_e/m$. K is Boltzmann's constant and e, m, n, T_e are the electronic charge, mass, number density and temperature respectively. When only the first two terms are included in equation (1a) it is usually known as the 'Bohm and Gross' dispersion relation (1949).

Laboratory experiments, however, are most frequently performed in cylindrical plasma columns immersed in strong axial magnetic fields; thus the theory must be modified to include both these features and, if necessary, particle collisions. Hence, in part I, we derive the dispersion relation for electron plasma waves propagating in an infinitely long, but radially bounded, cylindrical plasma immersed in a strong axial magnetic field and surrounded by vacuum. This shows that the dispersion of waves in terms of the wave number

component parallel to the magnetic field is modified by the finite radius a so that waves with $\lambda \geqslant a$ have frequencies below the plasma frequency and an approximately constant phase velocity: at much shorter wavelengths the dispersion is essentially that of infinite plasma. Because the dispersion of warm, finite plasma, is obtained as the solutions of a transcendental eigen-value equation, we present numerical solutions to this equation in a form which allows the dispersion and damping to be plotted for the lowest radial eigen-mode for arbitrary parameter a/λ_D. The computer program used to solve this equation is given in Appendix 2. Appendix 1 gives a simplified derivation of the plasma permittivity component parallel to a magnetic field, and Appendix 3 considers the effect of an axial density gradient on wave attenuation.

There is one other important point on which most laboratory experiments differ from the assumptions made in much of the published theory. Experiments are usually performed by continuously exciting a wave with a frequency ω by applying a sinusoidal voltage to a stationary probe immersed in the plasma. The resulting plasma fluctuations are detected by a receiving probe which can be moved away from the exciter, enabling the wavelength and spatial amplitude variation to be determined. Thus the experiment is usually concerned with the boundary value problem, where the angular frequency ω is taken to be real and the wave number $k = k_r + ik_i$ is complex, in contrast with theory which usually treats the initial value problem in which case $\Omega = \omega + i\gamma_L$ is complex and k is real. In Appendix 4 we show that for waves which are not too heavily attenuated $\gamma_L = - k_i \, d\omega/dk$, i.e. they are related by the wave group velocity.

In part II, after a brief description of the apparatus, we describe how waves are excited and detected and the experimental techniques used for measuring their wavelengths and spatial amplitude variations. Some experimental data are then presented and their interpretation discussed. Finally, in this section, we present experimentally determined dispersion and damping curves and show how they are used to establish the electron number density and temperature respectively.

The effect of electron-neutral particle collisions on wave damping is considered in Part III and non-linear effects are briefly discussed in Part IV.

PART I

THEORY

1.1 ELECTRON PLASMA WAVE PROPAGATION ALONG A STRONGLY MAGNETIZED PLASMA COLUMN

General expressions for the dispersion* and damping of waves propagating in warm, collisionless, magnetized plasma and whose wave vectors make arbitrary angles with the magnetic field vector are derived in several books [e.g. Montgomery and Tidman (1964) linearize Vlasov's and Maxwell's equations using perturbation theory and obtain solutions using integral transforms; Stix (1962), Clemmow and Dougherty (1969) and Krall and Trivelpiece (1973) solve the linearized equations by the method of integrating along unperturbed particle orbits]. Both approaches, which lead to the same result, are long and complicated and will not, therefore, be reproduced here. Rather, we note from their results that for frequencies $\omega \sim \omega_{pe}$ with $\omega_{pe} \ll \omega_{ce}$ (the electron cyclotron frequency $\omega_{ce} = eB_o/mc$ where B_o is the strength of a steady, uniform, applied magnetic field and c is the velocity of light) the plasma may be considered as a charge-free dielectric whose permittivity component perpendicular to the field is unity, so that for effects perpendicular to $\underline{B}_o$ the plasma behaves like a vacuum, while parallel to the field the permittivity is identical with that for unmagnetized plasma, and derive an eigen-value equation whose solutions describe wave propagation along a magnetized, radially bounded plasma. A simplified derivation of the permittivity parallel to $\underline{B}_o$ is given in Appendix I.

We suppose that there is no magnetic field associated with the wave in which case $\nabla \times \underline{E} = 0$ and the electric field distribution can be described by a scalar potential φ through

$$\underline{E} = -\nabla\varphi \quad . \qquad \ldots (3)$$

The principal limitation on the electrostatic approximation is $v_\varphi \ll c$.

The electric field must also satisfy Poisson's equation, which, for a charge-free dielectric, is

$$\nabla \cdot \underline{\underline{\epsilon}} \cdot \underline{E} = 0 \quad , \qquad \ldots (4)$$

where

$$\underline{\underline{\epsilon}} = \begin{bmatrix} \epsilon_{xx} & 0 & 0 \\ 0 & 1 & 0 \\ 0 & 0 & 1 \end{bmatrix}$$

---

* Strictly the word 'dispersion' includes damping because a dispersion relation, which describes the dependence of wave frequency ω on wave number k, is in general complex. However, 'dispersion' is frequently used to describe the real part of the relation only, while 'damping' refers to the imaginary part. In this report we use 'dispersion' and 'damping' in this sense.

is the plasma dielectric tensor, and

$$\epsilon_{xx} \equiv \epsilon = 1 - \frac{\omega_{pe}^2}{k^2 v_{Te}^2} Z'\left(\frac{\omega}{k v_{Te}}\right) . \qquad \ldots (5)$$

Equation (5) is derived in Appendix I. It is assumed that the electrons have a Maxwellian velocity distribution with a thermal velocity defined by

$$v_{Te} = \sqrt{\frac{2KT_e}{m}} . \qquad \ldots (6)$$

Using this definition $\omega_{pe} = v_{Te}/\lambda_D\sqrt{2}$. Z' is the derivative of the plasma dispersion function [Fried and Conte 1961].

We suppose the wave potential to vary like

$$\varphi(x,r,\theta) = \psi(r,\theta) \exp i(\omega t - kx) . \qquad \ldots (7)$$

Then

$$\underline{\nabla}\varphi = \hat{\underline{r}} \frac{\partial \varphi}{\partial r} + \hat{\underline{\theta}} \frac{1}{r} \frac{\partial \varphi}{\partial \theta} - i \hat{\underline{x}} k \psi \exp i (\omega t - kx) .$$

Because $\underline{\underline{\epsilon}}_{xyz}$ is of the form $\begin{pmatrix} \epsilon_{xx} & 0 \\ 0 & I_2 \end{pmatrix}$ it follows that

$$\underline{\underline{\epsilon}}_{xr\theta} \equiv \begin{pmatrix} \epsilon_{xx} & 0 \\ 0 & I_2 \end{pmatrix}$$

where I_2 is the unit 2×2 matrix and therefore

$$\underline{\underline{\epsilon}} \cdot \underline{\nabla}\varphi = \hat{\underline{r}} \frac{\partial \varphi}{\partial r} + \hat{\underline{\theta}} \frac{1}{r} \frac{\partial \varphi}{\partial \theta} - i \hat{\underline{x}} \epsilon k \psi \exp i (\omega t - kx) .$$

Because $\underline{\nabla} \cdot \underline{\underline{\epsilon}} \cdot \underline{\nabla}\varphi = 0$ then φ must satisfy

$$\underline{\nabla} \cdot \underline{\underline{\epsilon}} \cdot \underline{\nabla}\varphi = \frac{\partial^2 \varphi}{\partial r^2} + \frac{1}{r} \frac{\partial \varphi}{\partial r} + \frac{1}{r^2} \frac{\partial^2 \varphi}{\partial \theta^2} - \epsilon k^2 \varphi = 0 . \qquad \ldots (8)$$

Equation (8) is solved by separating the variables. Thus

$$\varphi(r,\theta,x,t) = R(r)\, \Theta(\theta) \exp i(\omega t - kx) ,$$

where R and Θ satisfy the equations

$$r^2 \frac{d^2R}{dr^2} + r \frac{dR}{dr} - (\epsilon k^2 r^2 + n^2) R = 0 \qquad \ldots (9)$$

and

$$\frac{d^2\Theta}{d\theta^2} = - n^2 \Theta . \qquad \ldots (10)$$

For the case where ϵ is not a function of r (i.e. the plasma is radially uniform*) equation (9) is the modified Bessel equation which has solutions [see, e.g. Sneddon 1961, pp.126-128]

$$R = A I_n(\sqrt{\epsilon}\, kr) + B K_n(\sqrt{\epsilon}\, kr) ,$$

where I_n and K_n are n^{th} order modified Bessel functions of the first and second kinds respectively.

---

* The case of a parabolic density variation leads to parabolic cylinder functions and the consequent modification to the dispersion relation at long wavelengths is discussed by Barrett, Jones and Franklin (1968).

As $r \to 0$, $K_n \to \infty$ thus inside the plasma $B = 0$ and the solution to equation (8) is

$$\begin{aligned} \varphi_{inside} &= AI_n(\sqrt{\epsilon}\,kr)\exp(in\theta)\exp i(\omega t - kx) \\ &= AJ_n(i\sqrt{\epsilon}\,kr)\exp(in\theta)\exp i(\omega t - kx) \end{aligned} \qquad \ldots (11)$$

where J_n is the n^{th} order Bessel function of the first kind.

If we suppose that the plasma column is surrounded by vacuum ($\epsilon = 1$) with no conducting surfaces nearby, then outside the plasma $A = 0$, since $I_n \to \infty$ as $r \to \infty$, and the solution to equation (8) is

$$\varphi_{outside} = BK_n(kr)\exp(in\theta)\exp i(\omega t - kx) \qquad \ldots (12)$$

The two solutions (11) and (12) must be matched at the boundary using the condition that the tangential components of $\underline{E}$ (i.e. E_θ and E_x) and the normal component of $\underline{D}$ (i.e. D_r) are continuous across the boundary.

Equating the partial derivatives with respect to x of equations (11) and (12) at $r = a$ gives

$$-k\,AJ_n(i\sqrt{\epsilon}\,ka)\exp(in\theta) = -k\,BK_n(ka)\exp(in\theta) \qquad \ldots (13)$$

and equating the partial derivatives w.r.t. r at $r = a$ gives

$$i\sqrt{\epsilon}\,k\,AJ_n'(i\sqrt{\epsilon}\,ka)\exp(in\theta) = k\,BK_n'(ka)\exp(in\theta) \qquad \ldots (14)$$

Dividing (13) by (14) gives

$$\frac{J_n(i\sqrt{\epsilon}\,ka)}{i\sqrt{\epsilon}\,J_n'(i\sqrt{\epsilon}\,ka)} = \frac{K_n(ka)}{K_n'(ka)} \equiv \frac{H_n^{(1)}(ika)}{H_n^{(1)\prime}(ika)}\,, \qquad \ldots (15)$$

where $H_n^{(1)}$ is the n^{th} order Hankel function of the first kind. This eigen-value equation was first derived by Gould (1964). Its solutions give ϵ as a function of ka for various mode numbers n. Values of ϵ can then be substituted into equation (5), which can be written

$$\epsilon(\omega,k) = 1 - \left(\frac{\omega_{pe}a}{v_{Te}}\right)^2 \left(\frac{1}{ka}\right)^2 Z'\left(\frac{\omega}{\omega_{pe}} \cdot \frac{\omega_{pe}a}{v_{Te}} \cdot \frac{1}{ka}\right)\,, \qquad \ldots (16)$$

which is then solved for ω/ω_{pe} for given values of $\omega_{pe}a/v_{Te}$.

The text of an ALGOL program to solve equation (15) is given in Appendix 2.

The curves shown in Figs.1 to 4 were calculated using this program, and are for electron plasma waves propagating in a radially uniform, collisionless ($\nu/\omega_{pe} = 0$) plasma column (remote from any conducting surfaces) in the $m = 1, n = 0$ mode (m is the m^{th} zero of the n^{th} order Bessel function of the first kind) i.e. in the lowest order radial azimuthally symmetric or fundamental mode. Using Figs.1 and 2 dispersion curves for any value of $\omega_{pe}a/v_{Te}$ ($= a/\lambda_D\sqrt{2}$) can be obtained for $\omega \leq 1.2\,\omega_{pe}$. Fig.1 gives ka as a function of $\omega_{pe}a/v_{Te}$ for values of ω/ω_{pe} in the range $0.5 \leq \omega/\omega_{pe} \leq 1.05$. Clearly,

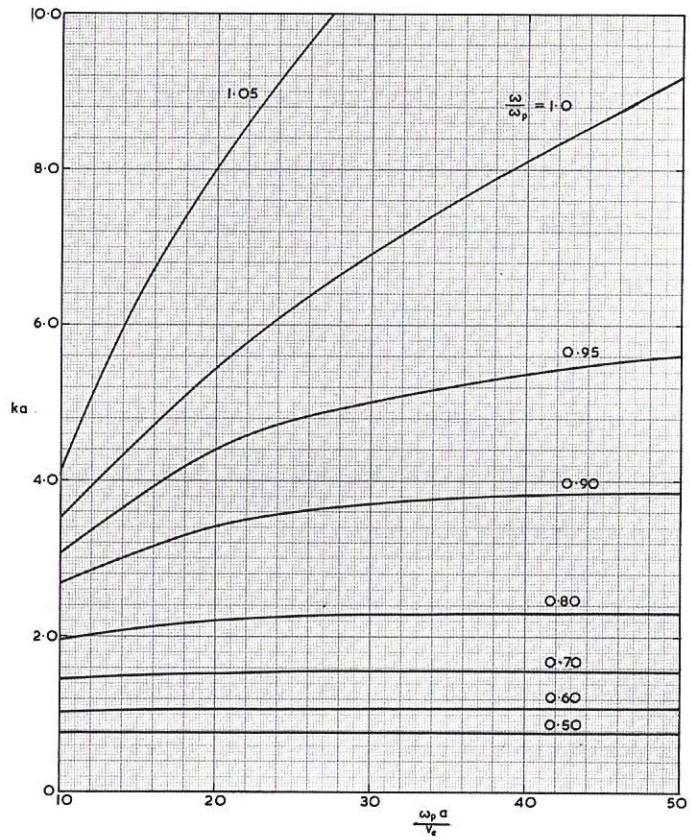

Fig.1
ka versus $\omega_{pe}a/v_{Te}$ with ω/ω_{pe} as parameter

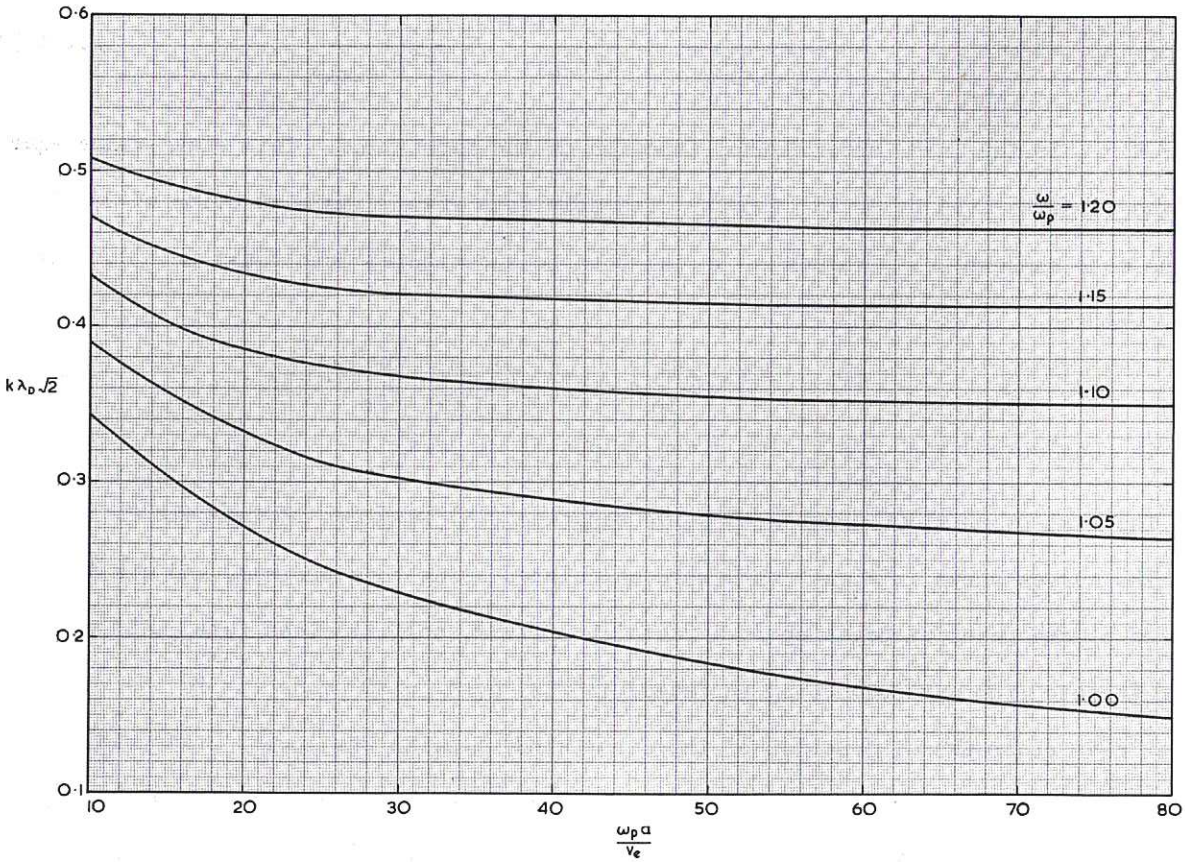

Fig.2
$k\lambda_D\sqrt{2}$ versus $\omega_{pe}a/v_{Te}$ with ω/ω_{pe} as parameter

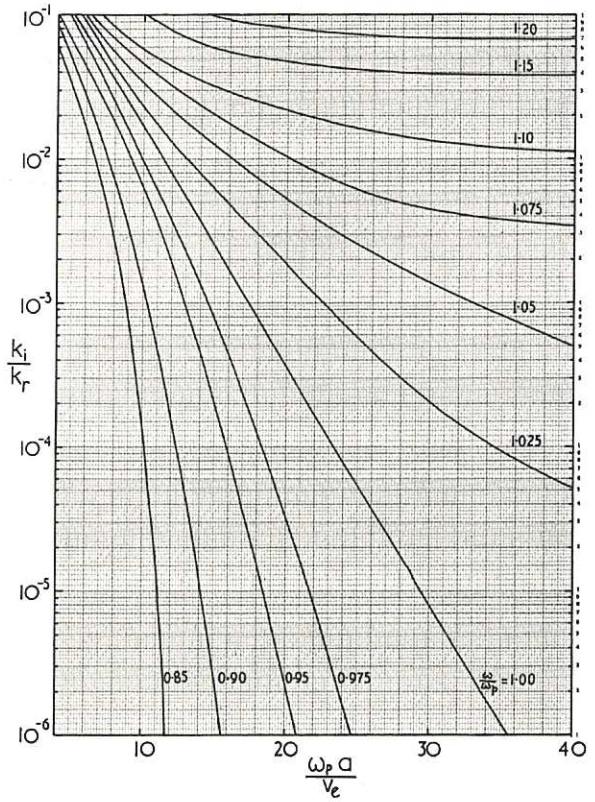

Fig.3
k_i/k_r versus $\omega_{pe}a/v_{Te}$ with ω/ω_{pe} as parameter

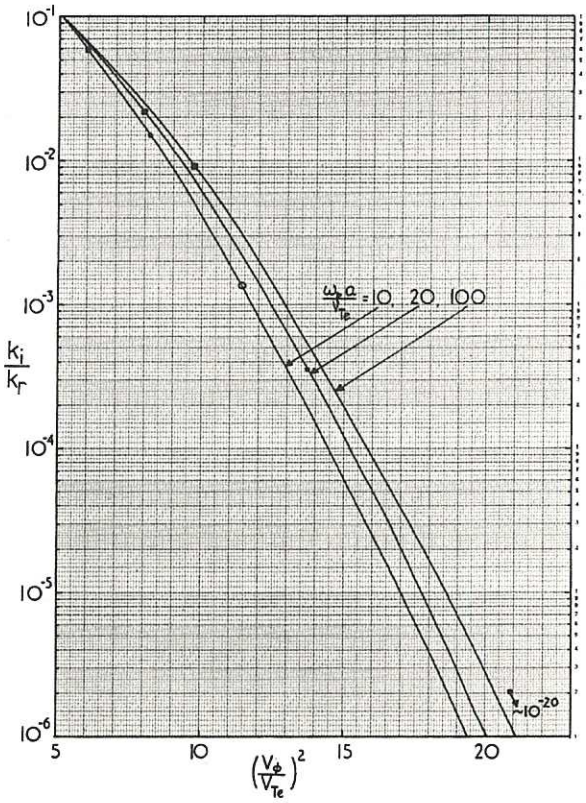

Fig.4
k_i/k_r versus $(v_\varphi/v_{Te})^2$ with $\omega_{pe}a/v_{Te}$ as parameter; ■ 1.1 ω_{pe} ; ● ω_{pe} ; ○ 0.9 ω_{pe}

when $\omega > \omega_{pe}$, k is not conveniently normalized to a ; it is more suitable to use λ_D. Thus Fig.2 shows $k\lambda_D\sqrt{2} = (ka)/(\omega_{pe}a/v_{Te})$ as a function of $\omega_{pe}a/v_{Te}$ for $1.0 \leq \omega/\omega_{pe} \leq 1.2$.

Damping curves are obtained from the curves shown in Fig.3 which give values of k_i/k_r as a function of $\omega_{pe}a/v_{Te}$ for values of ω/ω_{pe} in the range 0.85 to 1.2. Fig.4 shows k_i/k_r as a function of the square of the wave phase velocity normalized to the electron thermal velocity, i.e. $(v_\varphi/v_{Te})^2$ for $\omega_{pe}a/v_{Te}$ = 10, 20 and 100. This figure clearly illustrates that k_i/k_r varies very rapidly with v_φ/v_{Te} but, for the range of normalized phase velocities shown, is relatively insensitive to the ratio a/λ_D. The damping of waves at the plasma frequency is shown by the solid dots, while that at 0.9 ω_{pe} and 1.1 ω_{pe} is shown by an open circle and solid squares respectively.

An approximate dispersion relation for electron plasma waves propagating with phase velocities $v_\varphi \ll c$ in a warm electron plasma which completely fills a cylindrical waveguide immersed in a strong axial magnetic field is [see, e.g. Krall and Trivelpiece 1973, p.170]

$$\left(\frac{\omega}{\omega_{pe}}\right)^2 = \frac{k^2a^2}{k^2a^2 + p_{mn}^2} + \frac{3}{2}\,\frac{k^2a^2}{(\omega_{pe}a/v_{Te})^2} \qquad \ldots (17)$$

where p_{mn} is the m^{th} zero of the n^{th} order Bessel function of the 1st kind. This relation, or its cold plasma form (first term on r.h.s. only) is frequently used to describe the high frequency dispersion of plasma which partly fills a waveguide, as does ours. Generally, it does not give an accurate description of our data, although its shape is similar to that measured.

PART II

EXPERIMENTAL

2.1 THE PLASMA

The experiments are performed on a thermally ionized, sodium plasma column, radially confined by a strong (1 - 5 kG) uniform, axial magnetic field. The experimental arrangement is shown schematically in Fig.5. Access to the plasma is either by radial probes which can be moved along the axis of the column, or by four radially moving probes half-way along the plasma column.

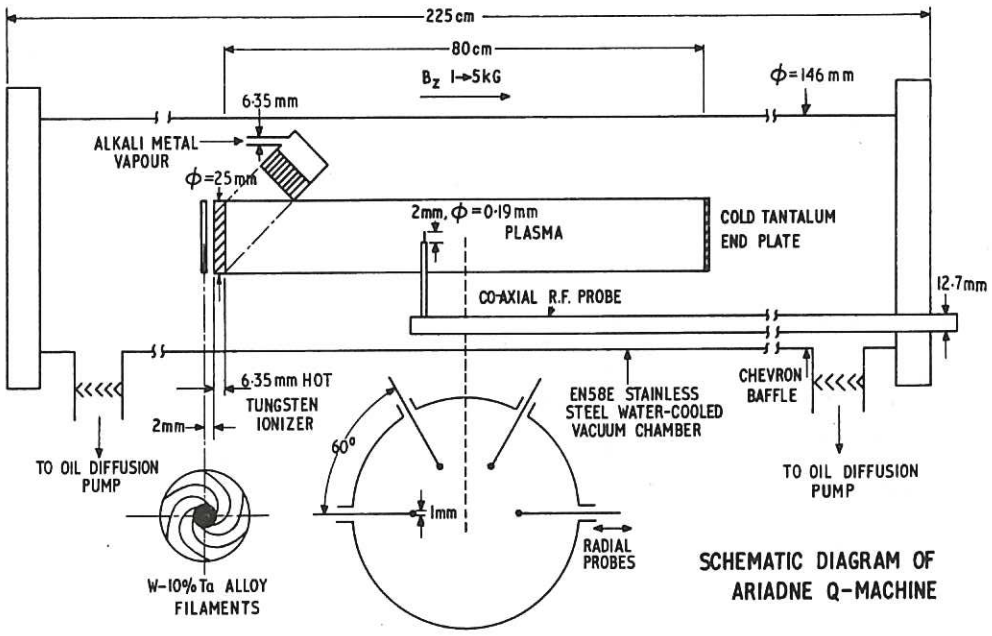

Fig.5
Arrangement of ARIADNE Q-machine

Plasma is synthesized in a watercooled ($\sim 15^{\circ}C$), evacuated (background pressure $\leq 1 \times 10^{-6}$ torr) stainless steel tube, internal diameter 15 cm, at a single earthed tungsten plate 6 mm thick, 25 mm diameter and heated by electron bombardment on its back surface. The temperature T of the front surface can be maintained between 2200 K and 2600 K and, by using specially shaped (spiral) filaments as the source of bombarding electrons [Burt, Little and Stott 1969] is kept uniform to within 50 K. The electrons are produced by thermionic emission and the ions by surface ionization of a beam of sodium vapour produced in an oven and uniformly directed onto the hot tungsten plate by a collimator, diameter 20 mm, consisting of multiple capilliary tubes each 1 mm diameter. Because it is not usual to achieve an appropriate balance between the flux of electrons and ions leaving the ionizing surface there is in general a space charge sheath in front of the hot plate [Ott 1967; Tropmann 1970]; observations show the plasma is most quiet when the sheath is slightly electron rich, and all our measurements are made under these conditions.

The column is terminated 80 cm from the hot plate by a cold, plane, tantalum disk which, because its potential is allowed to float, reflects all but the fastest electrons (i.e. those with energies $\geq 10 KT_e$) ; thus the electron velocity distribution function is essentially a full one-dimensional Maxwellian with the same temperature as the hot plate. The ions, however, because they are accelerated through the electron-rich sheath at the hot plate have a net drift towards the cold plate where they are absorbed. Their velocity distribution function may be approximated to a Maxwellian truncated to zero for velocities below some critical value $v_c \leq 2(2KT/M)^{\frac{1}{2}}$ where M is the ion mass [Buzzi, Doucet and Gresillon 1969; 1970; Andersen, Jensen, Michelsen and Nielsen 1971].

For the range of plasma conditions used, typically electron number density n between 1×10^7 and 3×10^8 cm^{-3}, electron temperature $T_e \sim 2500$ K, Langmuir probe measurements show that the axial density varied by less than 1%, consistent with very small losses by radial diffusion and volume recombination. This is illustrated in Fig.6 which shows the variation in the saturation ion current to a cylindrical Langmuir probe (which is directly proportional to ion density [Chen, Etievant and Mosher 1968]) moved along the plasma axis. The radial density dependence measured half-way between the hot and cold electrodes is shown in Fig.7a: the density is essentially constant over the area of the ionizing surface and falls rapidly beyond its edge. The fractional r.m.s. density fluctuation level $\delta n/n_o$, where n_o is the density on the axis, measured in a band 100 Hz to 50 kHz is shown in Fig.7b and is ~ 0.01 inside the plasma, rising to ~ 0.03 at its edge. The spectral distribution of these density fluctuations, shown in Fig.8, is a continuum concentrated mainly below ~ 20 kHz with an inverse frequency dependence closely resembling the 'flicker' noise observed in other thermionic devices [see, e.g. Robinson 1962] with a superimposed line spectrum which, from

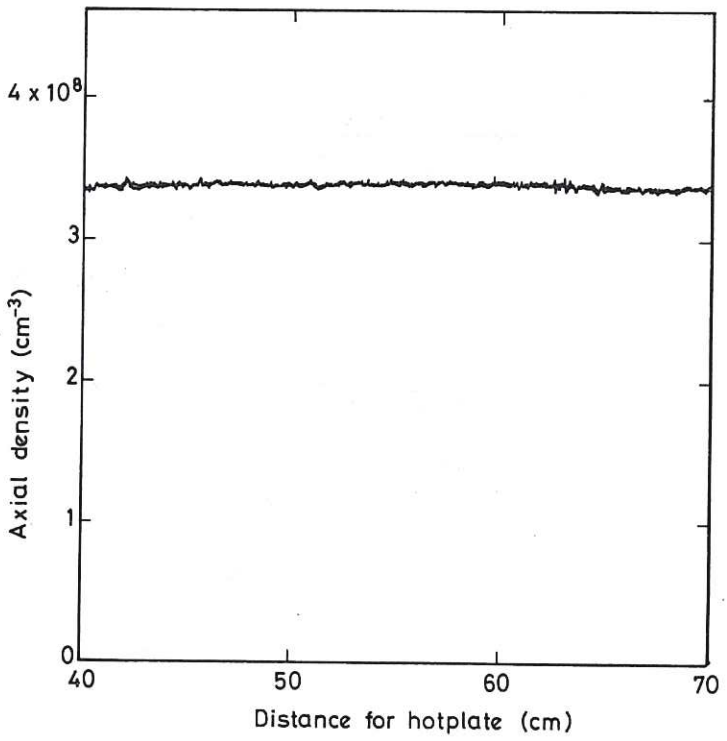

Fig.6
Saturation ion current to a cylindrical Langmuir probe moving along the axis of the plasma column

its dependence on magnetic field strength, is believed to arise from Kelvin-Helmholtz instabilities driven by the column rotation. This low frequency noise, although very weak, may have important effects on the accuracy of damping measurements when working with short wavelengths and very narrow bandwidth receivers [Franklin, Hamberger and Smith 1973].

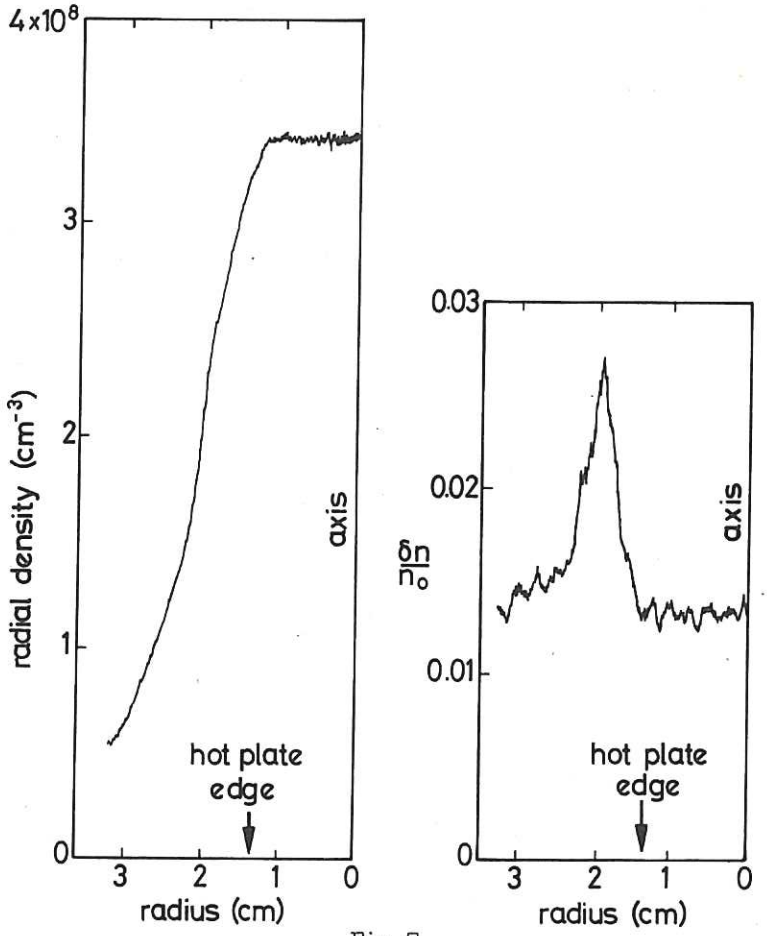

Fig.7
(a) Saturation ion current to a cylindrical Langmuir probe moving radially across the plasma 40 cm from the ionizing surface; (b) Radial variation in r.m.s. amplitude of fluctuations in band 100 Hz - 50 kHz in the saturation ion current shown in (a)

For typical operating conditions $n \simeq 3 \times 10^7$ cm^{-3} and $T_e = 2500$ K : thus $\lambda_D = 6.3 \times 10^{-2}$ cm, $a/\lambda_D \simeq 20$ and the number of electrons in a Debye sphere $N_D \simeq 3 \times 10^4$. The ratio of the electron-ion collision frequency, ν_{ei}, to the electron plasma frequency is $\sim 10^{-4}$ as can be shown from the expression given by Silin (1960) for ν_{ei} in the presence of a strong magnetic field ($\omega_{ce} \gg \omega_{pe}$)

$$\nu_{ei} = \frac{4}{3}\left(\frac{2\pi}{m}\right)^{\frac{1}{2}} \frac{ne^4}{(\kappa T_e)^{\frac{3}{2}}} \ell n \left(\frac{\Lambda}{3}\frac{\omega_{pe}}{\omega_{ce}}\right)$$

$$= 0.088 \frac{\omega_{pe}}{N_D} \ell n(3 N_D \omega_{pe}/\omega_{ce}) \quad \ldots (18)$$

where

$$\Lambda = \frac{3}{2e^3}\left(\frac{\kappa^3 T_e^3}{n\pi}\right)^{\frac{1}{2}} = 9 N_D .$$

Thus we may consider the medium as an essentially collisionless plasma.

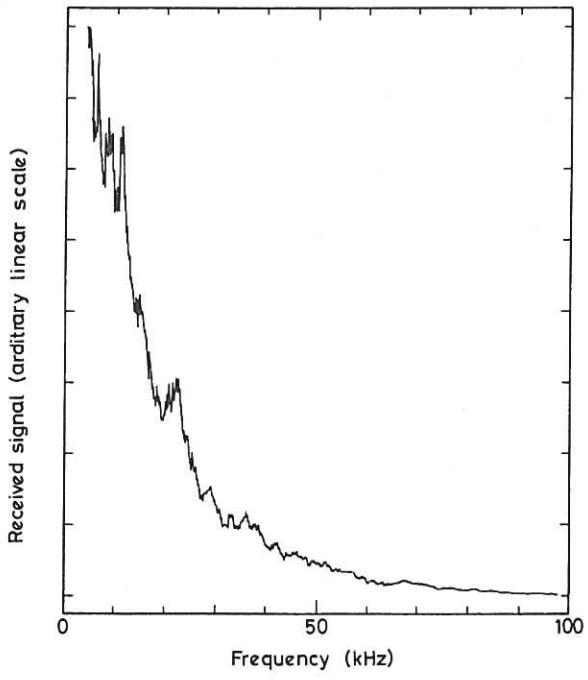

Fig.8
Spectrum of fluctuations in saturation ion current to a cylindrical Langmuir probe on the axis of the plasma column

Spatial variations in the strength of the confining magnetic field are less than 0.5% on its axis, which is co-linear to within ± 1 mm with the axes of the vacuum tube and plasma column.

2.2 WAVE EXCITATION AND DETECTION

Waves are excited by applying small, high frequency, sinusoidal voltages (< 100 mV) from a signal generator to a short, fine platinum wire radial electrode (~2 mm long and 0.2 mm diameter) located at a fixed position on the axis of the plasma column, the connection being made by 50 Ω semi-rigid coaxial transmission line terminated by a matching 50 Ω disk resistor near the probe tip. The probe construction is shown in Fig.9. The alternating signal perturbs the plasma, resulting in the excitation of electron plasma waves: at frequencies above ω_{pe} all the modes have short wavelengths and higher order modes have lower phase velocities than that of the fundamental. This means that the greater Landau damping of the higher order modes ensures that the wave field is that of the lowest order radial, and azimuthally symmetric, mode, within a few wavelengths of the transmitter. At lower frequencies higher order modes may also be excited as propagating waves.

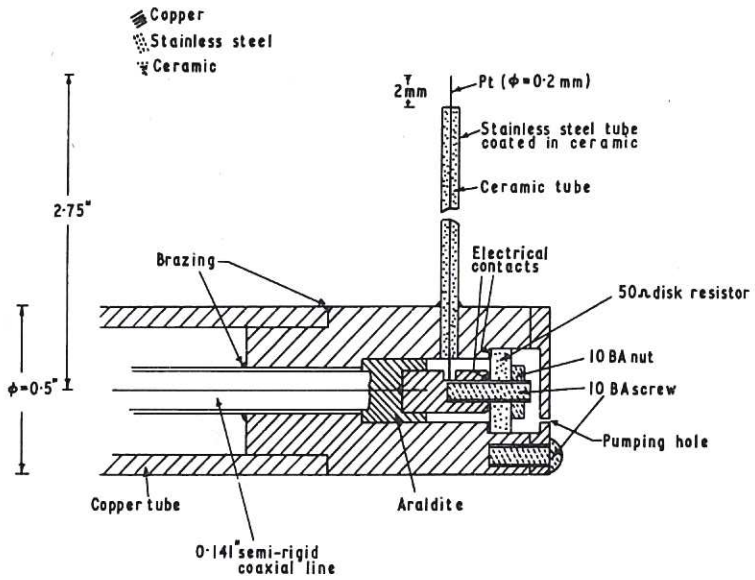

Fig.9
Construction of transmitting probe

Detection of waves is by a similar probe, but without the disk resistor, also located on the plasma axis, and connected to radio-frequency apparatus suitable for measuring the phase and relative amplitude of the alternating plasma potential component at the wave frequency ω as it moves along the whole length of the plasma column at a speed $\sim 5\,\mathrm{mm\,s^{-1}}$. Sometimes, when absolute measurements of the wave amplitude are required, the coupling of the probe to the plasma is improved by connecting a high input impedance FET amplifier close to the probe tip.

Coupling between the probes and the plasma is weak: typically the wave potential is ~0.01 of the potential applied to the transmitting probe and the potential measured with the receiving probe is ~0.01 of the wave potential. Direct electromagnetic coupling between the transmitting and receiving probes is entirely by the induction field because at the wave frequencies used (20-200 MHz) the metal vacuum tube behaves as a cut-off waveguide, and is negligible (≤ -90 dB) when the separation of the two probes exceeds about 10 cm.

2.3 MEASUREMENT OF WAVELENGTH AND DAMPING LENGTH

Wavelengths are determined by comparing the phase of the detected signal as a function of probe separation with that of a fixed reference signal, and damping lengths by measuring its spatial amplitude variation using a calibrated receiver. Two techniques are used, depending on the available measurement apparatus. In one the high frequency wave signal is 100% amplitude modulated with a square wave at a low frequency (1 kHz) and the amplitude of the demodulated signal measured; in the other the high frequency signals themselves are measured directly. For a given frequency both the wavelength and damping length are measured simultaneously; this reduces experimental uncertainty because it eliminates the need to allow for small variations in phase velocity and consequently larger significant changes in attenuation [which depends exponentially on the ratio $(v_\varphi/v_{Te})^2$] arising from small changes in the plasma conditions (e.g. density) which can occur between consecutive measurements taken a few minutes apart.

2.3.1 Modulation Technique

A block diagram of the arrangement is shown in Fig.10. The modulated high frequency signal is applied to the transmitter probe through a d.c. isolator, a sample being taken using a 10 dB directional coupler (Anzac DCG-10) and used as the interferometer reference signal. Because the line is correctly matched near the probe a high impedance valve voltmeter anywhere across the line measures the potential applied to the probe tip. The detected signal passes through a high pass filter (> 11 MHz) which prevents low frequency

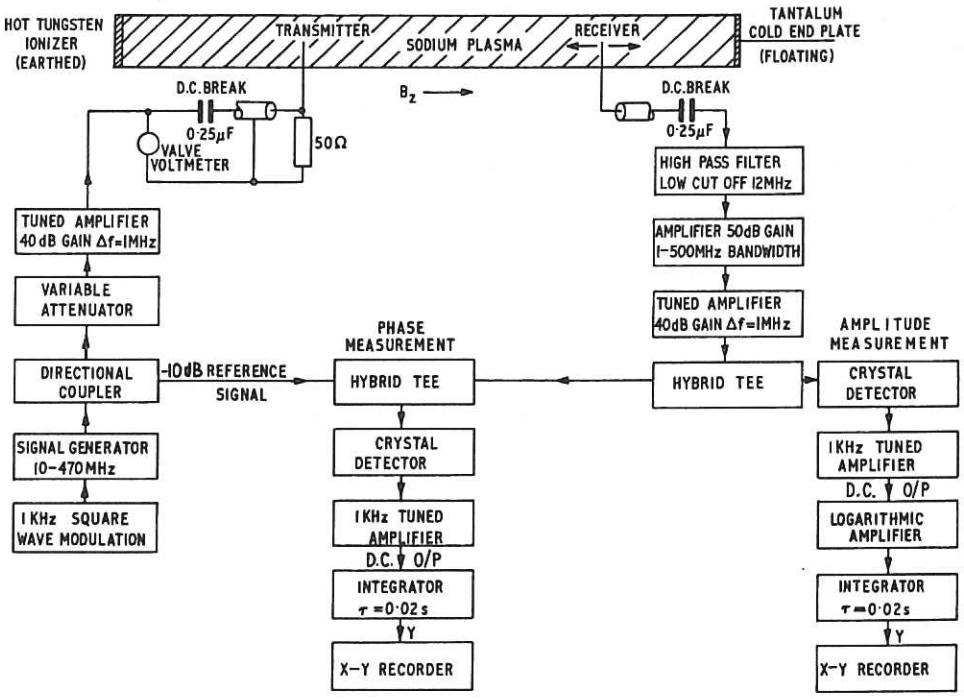

Fig.10
Arrangement for measuring wavelength and spatial attenuation of propagating electron plasma waves using modulation technique

plasma noise entering subsequent electronics, and is amplified by a low noise, broad-band amplifier (Avantek UAA-326 B) followed by a tuned amplifier (bandwidth $\Delta f \simeq 1$ MHz) (Hewlett-Packard 230A), whose output is split by a hybrid junction (Anzac T-1000), one part being used to measure wavelength, the other to measure attenuation.

First consider wavelength measurements. The plasma signal and the reference signal (for best results the reference is adjusted to be ~ 5 dB above the plasma signal) are added vectorially in a hybrid junction and rectified and demodulated in a square law r.f. crystal detector (Hewlett-Packard 8471 A) the output of which contains a component at the modulation frequency proportional to $\varphi_o e^{-k_i x} \cos kx$, where φ_o is the amplitude of the wave at the transmitter. This component is amplified in a narrow-band (~ 20 Hz) amplifier (Hewlett-Packard 415 E) tuned to the modulation frequency, rectified, smoothed and used for the vertical deflection of an x-y recorder (Bryans 26000), the horizontal axis being proportional to the probe separation. The wavelength is then measured directly from this trace.

To measure the relative amplitudes of the wave at different positions along the column the amplifier output is rectified and filtered in a second r.f. detector to produce a signal component at the modulation frequency proportional to the local amplitude of the wave. This is amplified by a second narrow-band tuned amplifier, rectified, smoothed, logarithmically amplified and finally used for the vertical deflection of a second x-y recorder. A suitable time constant ($\tau = 0.02$ s) integrator removes any faster fluctuations from the recorder trace. The vertical deflection is calibrated directly from the signal generator using a standard attenuator. For typical conditions the deflection is logarithmic for a 25 dB range. For a wave whose amplitude falls exponentially with distance the trace on the x-y recorder is a straight line whose slope is proportional to damping length. The damping is related to the slope of the trace by

$$\frac{k_i}{k_r} = 1.83 \times 10^{-2}\, m\lambda \qquad \ldots (19)$$

where m is the slope (in dB/cm) and λ the wavelength (in cm), both measured from the traces. Linearity of the trace implies great constancy of number density with distance as shown in Appendix 3.

2.3.2 C.W. Measurement

The experimental arrangement is shown in Fig.11. Measurement of wavelength is essentially the same as in 2.3.1 except that the phases are compared directly using a balanced mixer (Anzac ASM-10) whose output is proportional to $\cos kx$. The wave amplitude is measured directly using a spectrum analyzer (Hewlett-Packard 8553B/8552B/141T) in the unswept

mode and operating as a narrow-band (1-300 kHz) receiver tuned to the wave frequency, and whose ouput is proportional to the logarithm of the original signal. k_i/k_r is found as above.

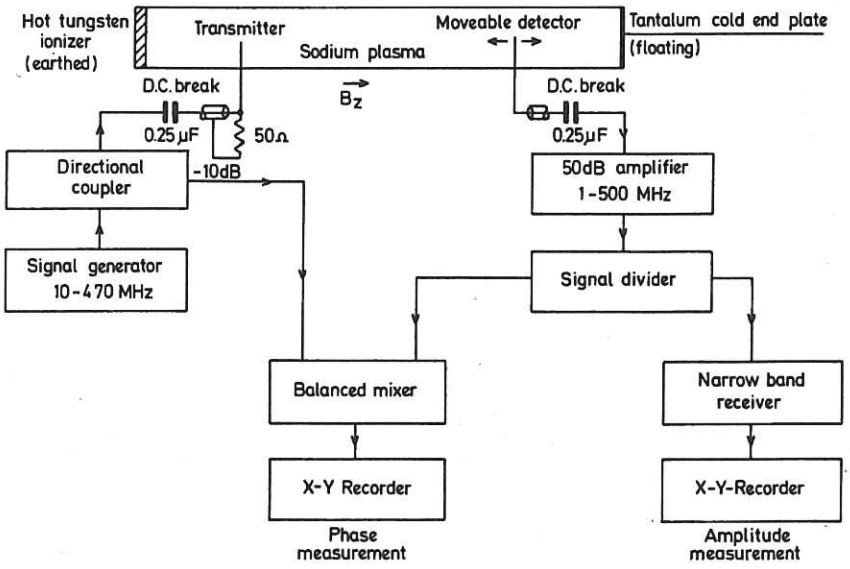

Fig.11
Arrangement for measuring wavelength and spatial attenuation of propagating electron plasma waves using c.w. method

The dynamic range is considerably increased by using a very narrow bandwidth receiver (50-300 Hz) to improve the signal-to-noise ratio, in conjunction with a (tracking) generator (Hewlett-Packard 8443B) whose frequency is locked to that of the receiver. However, some care must be exercised, particularly for the shortest wavelengths where Landau damping is greatest, to ensure that the relative amplitude measurements are independent of receiver bandwidth. Low frequency density fluctuations modulate the phase and amplitude of the wave and can, if the receiver bandwidth is too narrow, displace wave energy to frequencies outside the response of the receiver, in which case an exaggerated damping is measured [Franklin, Hamberger and Smith 1973]. These fluctuations in phase of the received signal also prevent wave damping from being measured directly from the wave pattern produced by the interferometer, since this strictly measures the phase correlation between the received signal and the reference. This phase correlation length is in general less than the damping length appropriate to the amplitude of the plasma wave.

2.4 EXPERIMENTAL DATA

Figure 12 shows typical experimental recordings. The lower trace shows the variation in output from the interferometer as the probe separation increases, from which the wavelength (phase velocity) is determined. The upper trace shows the relative amplitude of the detected signal as a function of probe separation. Clearly, over much of this trace the wave amplitude decays exponentially, as predicted by linear theory. However, when the transmitter and detector probes are very close (within 8 cm) direct coupling between them

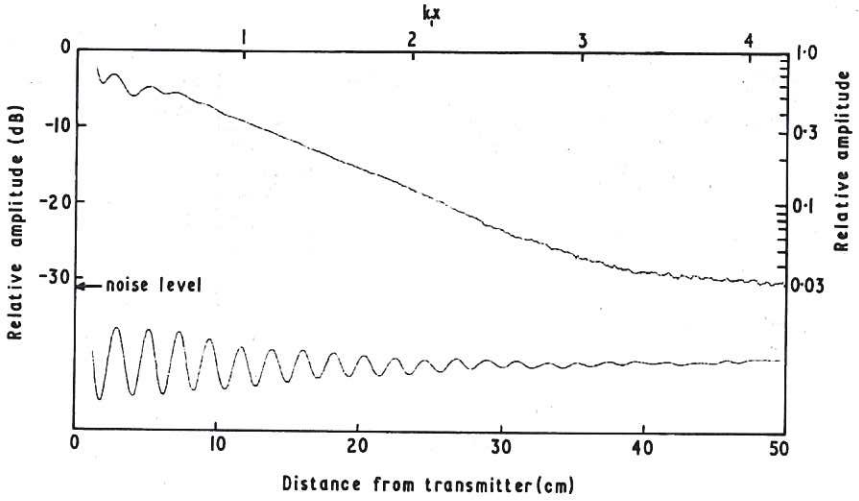

Fig.12
Raw experimental data showing (upper) relative spatial amplitude and (lower) relative phase of the received signal $\omega/2\pi = 33$ MHz , $k_r = 2.87$ cm^{-1} , $k_i/k_r = 2.95 \times 10^{-2}$ initial amplitude $\simeq 0.5$ mV . $n_e = 1.2 \times 10^7$ cm^{-3} , $T_e = 2350$ K, $a/\lambda_D = 14$. Receiver bandwidth $\Delta f = 1$ kHz

results in interference between the plasma and direct signal, i.e. the system acts as an interferometer; this produces oscillations with the same wavelength as in the lower trace. When the signal approaches the noise level of the receiver its damping departs from exponential: this instrumental effect is readily distinguished from genuine departures from exponential decay (arising, for example, from non-linear effects; see section 4 and Franklin, Hamberger and Smith 1972) by reducing bandwidth Δf. This is illustrated in Fig.13. In the lower traces the signal decreases exponentially for $\Delta f = 300$ Hz , when the signal is always well above the noise level (i), but appears to deviate from exponential for $\Delta f = 30$ kHz when the noise level is too high (ii). For both upper traces (iii) the initial amplitude of the wave has been increased by 10 dB : the signal is now always well above the noise levels for both bandwidths used ($\Delta f = 1$ kHz and 100 kHz) and the decay is independent of Δf ; this confirms that the non-exponential decay in this case is a real effect caused by the plasma non-linearity.

A typical result for a more lightly damped wave is shown in Fig.14. Although there is clearly an exponential decay, there are in addition oscillations with wavelength half that shown by

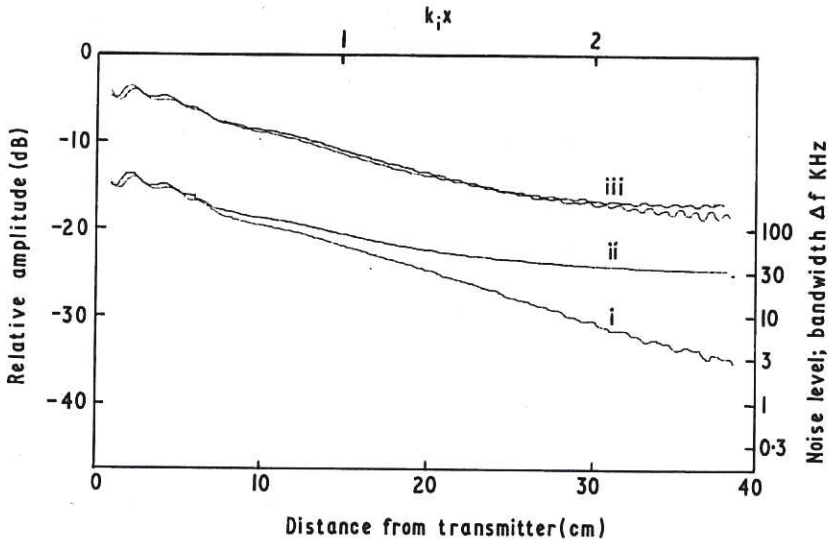

Fig.13
Raw experimental data showing relative spatial amplitude of (i) a small amplitude wave when receiver bandwidth $\Delta f = 0.3$ kHz ; (ii) the same wave as in (i) but for $\Delta f = 30$ kHz and (iii) the same wave but with initial amplitude increased by 10 dB and $\Delta f = 1$ kHz and 100 kHz. $\omega/2\pi = 36$ MHz , $k_r = 2.92$ cm^{-1} , $k_i/k_r = 2.2 \times 10^{-2}$. $n_e = 1.44 \times 10^7$ cm^{-3} , $T_e = 2500$ k , $a/\lambda_D = 14.8$

the interferometer. This effect occurs when the amplitude of the wave reflected by the cold plate is not negligible compared with that of the incident wave, and is not seen, of course, for heavily damped waves (as in Fig.12).

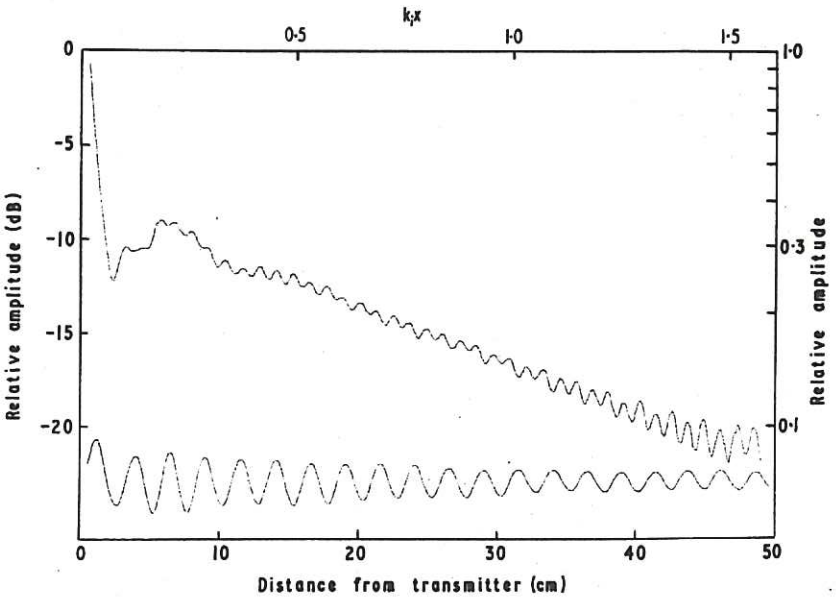

Fig.14
Raw experimental data showing (upper) relative spatial amplitude and (lower) relative phase of the received signal $\omega/2\pi = 31$ MHz, $k_r = 2.54\ cm^{-1}$, $k_i/k_r = 1.27 \times 10^{-2}$, initial amplitude $\simeq 0.5$ mV. $n_e = 1.2 \times 10^{7}\ cm^{-3}$, $T_e = 2350$ K $a/\lambda_D = 14$. Receiver bandwidth $\Delta f = 1$ kHz

Such effects limit the range over which reliable amplitude measurements can be made. For damping $\geqslant 5$ dB cm^{-1} the plasma signal is too weak to measure when the receiver is sufficiently far from the transmitter for direct coupling to be negligible. This limit can be overcome only by improving the plasma-wave/probe coupling relative to the direct electromagnetic signal. The reflections effectively prevent amplitude measurements being made for waves which attenuate by less than ~ 3 dB along the column. In practice normalized damping lengths can be measured in the range $10^{-1} \leqslant k_i/k_r \leqslant 10^{-3}$.

2.5 MEASURED DISPERSION AND DAMPING CURVES

The longest wavelength that can be studied is limited by the generation of higher order modes, which occurs when the wavelength of the fundamental exceeds the plasma radius, and the shortest is limited by wave damping. The range of frequencies for which wavelengths can be measured is $0.4 \leqslant \omega/\omega_{pe} \leqslant 1.3$.

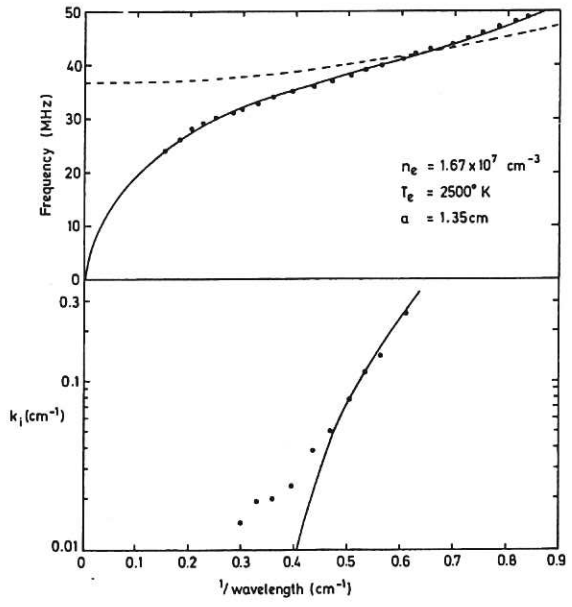

Fig.15
Measured dispersion and damping of propagating electron plasma waves with fitted theoretical curves. ---- Bohm and Gross equation

The measured dispersion and damping of electron plasma waves propagating in our plasma is shown in Fig.15 for one particular set of conditions. The experimental points have typical uncertainties $\Delta\omega/\omega \sim \pm$ 0.2%, $\Delta k_r/k_r \sim \pm$ 1% and $\Delta k_i/k_r \leqslant \pm$ 10%.

The solid lines are theoretical curves which best fit the experimental points (the curve fitting procedure is described in section 2.6). The dashed curve is the Bohm and Gross dispersion relation for the fitted temperature and density. This clearly cannot describe our observations. At long wavelengths ($\lambda \geq a$) finite radius effects become important and allow propagation below the plasma frequency: physically this can be explained because the wave field extends beyond the plasma boundary which reduces the electrostatic coupling between the electrons and ions and hence lowers the natural frequency of oscillation of the electrons. At short wavelengths, because the higher order terms in the expansion, neglected in the Bohm and Gross approximation, are no longer small only the Landau solution (with a small correction for finite radius) is adequate.

Damping measurements are restricted to a fairly narrow range of frequencies ($0.9\,\omega_{pe} \leq \omega \leq 1.2\,\omega_{pe}$). Values of k_i are obtained over about one decade and agree well with collisionless theory only for the more heavily attenuated short wavelength waves where Landau damping is the dominant damping mechanism. The damping at longer wavelengths is thought to be mainly due to particle collisions and, though small, considerably exceeds the extremely weak Landau damping.

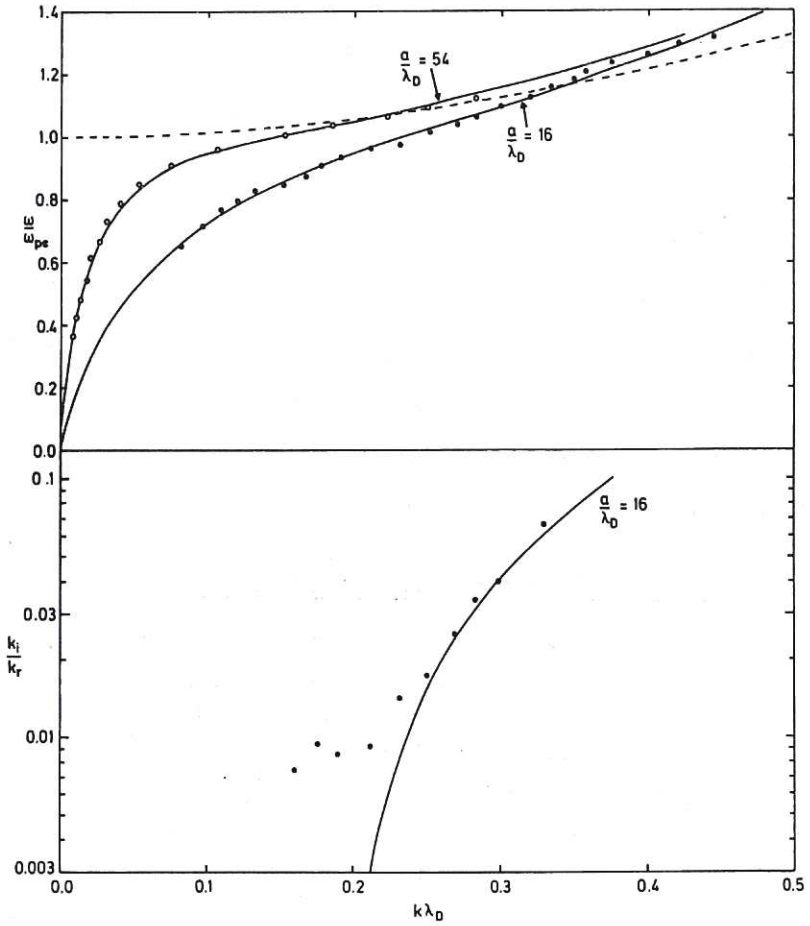

Fig.16
Normalized dispersion and damping measurements with fitted theoretical curves for electron plasma waves propagating in plasmas with the same temperature $T_e = 2500\,K$ but with differing densities; o $n_e = 3.38 \times 10^8\,cm^{-3}$, • $n_e = 1.67 \times 10^7\,cm^{-3}$

It is usually much more convenient to present data such as that of Fig.15 in normalized form: ω/ω_{pe} versus $k\lambda_D$ with a/λ_D as parameter. This produces curves which are easy to compare with theoretical dispersion curves. The upper part of Fig.16 shows some dispersion data plotted in this way: the solid dots are for the plasma of Fig.15 ($a/\lambda_D = 16$) while the open circles are for higher density plasma ($a/\lambda_D = 54$). Notice that for $k\lambda_D \geq 0.5$ both theoretical solid curves merge and become insensitive to a/λ_D; physically

this is because $\lambda \ll a$ and most of the wave field is confined to the plasma, making it appear unbounded. The dashed curve is the Bohm and Gross relation $(\omega/\omega_{pe})^2 = 1 + 3k^2\lambda_D^2$. The lower part of Fig.16 shows k_i/k_r versus $k\lambda_D$: the experimental points are again taken from Fig.15 and the theoretical curve is for $a/\lambda_D = 16$.

2.6 PROCEDURE FOR FINDING ELECTRON DENSITY AND TEMPERATURE

The propagation of electron plasma waves depends sensitively on both the electron density and temperature. By fitting theoretical curves, in a self-consistent manner, to their measured dispersion and damping both these important plasma parameters can be determined with high precision.

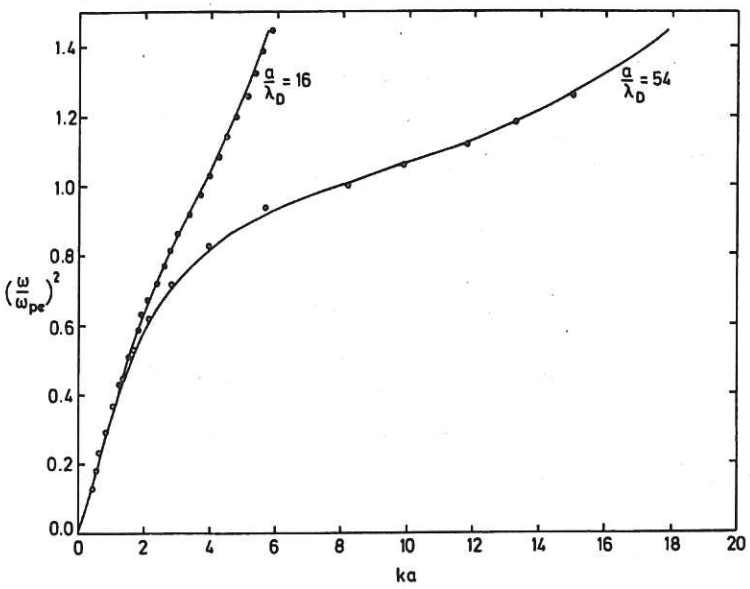

Fig.17
Dispersion curve for data presented in Fig.16 using alternative normalization

For the dispersion it is most convenient to use the alternative normalization shown in Fig.17 in which $(\omega/\omega_{pe})^2$ is plotted against ka, with a/λ_D as parameter. In this presentation the curves coalesce and become independent of a/λ_D at short wavelengths as in Fig.16. An examination of these curves shows that their slope is a minimum when $\omega = \omega_{pe}$.

For moderately damped waves the damping is given approximately by

$$\frac{k_i}{k_r} = \frac{2\sqrt{\pi}}{3}\left(\frac{v_\varphi}{v_{Te}}\right)^5 \exp\left[-\left(\frac{v_\varphi}{v_{Te}}\right)^2\right], \qquad \ldots (20)$$

and is not very sensitive to a/λ_D as shown in Fig.4. Thus we plot k_i/k_r against v_φ with T_e as parameter as in Fig.18.

The procedure used to determine n_e and T_e is as follows:

(1) Plot experimental values of ω^2 against k (to emphasize the slope near $\omega = \omega_{pe}$), put the value of ω at minimum slope equal to ω_{pe}.

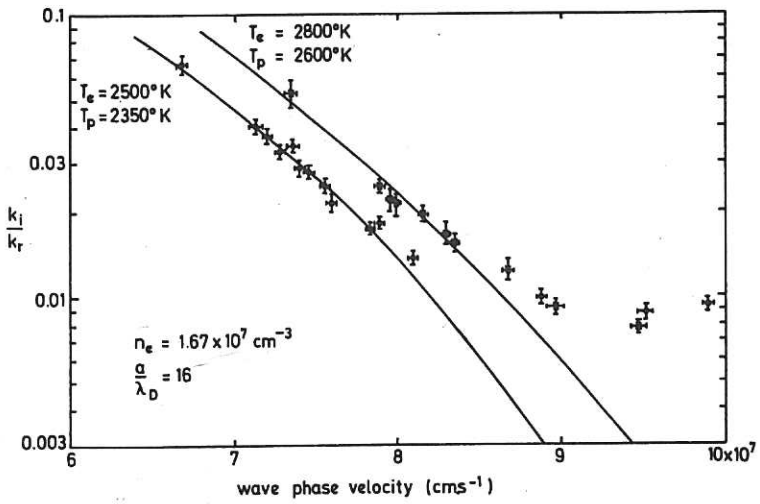

Fig.18
Normalized dampimg measurements and fitted theoretical curves for electron plasma waves propagating in plasmas with the same density but differing temperatures: • T_e = 2500 K, × T_e = 2800 K

(2) Replot data as $(\omega/\omega_{pe})^2$ versus k for long wavelengths ($\omega^2/\omega_{pe}^2 \leq 0.4$) and from its slope m find the effective radius of the plasma column given by $a = 3.04\,m$. (It should be close to the geometrical radius.)

(3) Take the measured hot plate temperature as T_e to find an approximate value for a/λ_D.

(4) Plot k_i/k_r against v_φ and using the approximate value of a/λ_D fit a theoretical curve to the experimental points. This gives a more accurate estimate for T_e and a/λ_D.

(5) Using this new value of a/λ_D plot $(\omega/\omega_{pe})^2$ versus ka and compare with theoretical curves as in Fig.17. If the original estimate for ω_{pe} was inaccurate the points for $(\omega/\omega_{pe})^2 > 1$ will not lie on the theoretical curve in which case a new estimate for ω_{pe} must be made.

(6) Using this new estimate of ω_{pe} repeat the procedure from (2).

This iterative procedure is continued until consistency between the theoretical curves, experimental points and the calculated value of a/λ_D is found. Usually two or three iterations are adequate to determine ω_{pe} (and hence n) and T_e to within a few percent ($\leq \pm 3\%$ for each).

The temperature of the electrons determined from the damping of electron plasma waves agrees with the temperature of the ionizing surface determined using an optical pyrometer to $\sim \pm$ 5% (see Fig.18). This is within the limits of experimental uncertainty of the pyrometric measurement due to unknown emissivity of the hot surface, window transmission etc.

Strictly we should remember that Landau damping is a measure of the slope of the electron distribution function at the phase velocity of the wave, and that we are ascribing the temperature to a distribution which we assume to be Maxwellian.

PART III

COLLISIONAL EFFECTS

Real plasma is never completely free from inter-particle collisions, although the collision frequencies can be much less than the wave frequency. To develop a theory which includes the effect of collisions on the wave propagation constants we assume that they can be described by the Bhatnagar, Gross and Krook (1954) model equation, in which case the electron distribution function satisfies

$$\frac{\partial f}{\partial t} + v\frac{\partial f}{\partial x} + \frac{eE}{m}\frac{\partial f}{\partial v} = -\nu(f - f_o) \ , \qquad \ldots (21)$$

where ν is an empirical collision frequency and f_o is a suitable Maxwellian distribution function. This equation is discussed by Clemmow and Dougherty (1969) where it is noted that it best describes collisions between charged and neutral particles and is less suitable for describing those between charged particles.

The dispersion and damping of electron plasma waves propagating along an axially magnetized plasma column can be found by numerically solving equation (15), collisional effects being included through an appropriate expression for the permittivity component parallel to the field. This we obtain by substituting the expression for space charge density given by Clemmow and Dougherty (equation 9.121), i.e.

$$\rho = -\frac{2ine^2 E_o\{1 + \zeta Z(\zeta)\}}{mv_{Te}^2 k\left\{1 + i\frac{\nu}{\omega}\cdot\frac{\omega}{kv_{Te}}Z(\zeta)\right\}} \qquad \ldots (22)$$

where $\zeta = \frac{\omega}{kv_{Te}}\left(1 + \frac{i\nu}{\omega}\right)$ and $G(z) \equiv G(-\zeta) \equiv Z(\zeta)$, into Poisson's equation which, for perturbations varying like $\exp[-i(\omega t - kx)]$ is

$$ik E_o = 4\pi\rho \ , \qquad \ldots (23)$$

to give

$$\epsilon(\omega,k) \equiv 1 + \frac{i\nu/\omega}{1 + i\nu/\omega}\zeta Z(\zeta) + \frac{2\omega_{pe}^2}{k^2 v_{Te}^2}\left\{1 + \zeta Z(\zeta)\right\} = 0 \ . \qquad \ldots (24)$$

Since $2\{1 + \zeta Z(\zeta)\} \equiv -Z'(\zeta)$, equation (24) clearly reduces to equation (5) when $\nu = 0$.

The computer program in Appendix 2 solves equation (15) for real ω and complex k with ν/ω_{pe} as parameter using expression (24) for $\epsilon(\omega,k)$. For values of $\nu/\omega_{pe} \leq 0.1$ the dispersion is almost identical with that for collisionless ($\nu/\omega_{pe} = 0$) plasma. However, k_i/k_r is strongly dependent on ν/ω_{pe} and can differ by orders of magnitude from the $\nu/\omega_{pe} = 0$ case. Some representative results are shown in Fig.19 where for each value of ω/ω_{pe} we plot k_i/k_r against $\omega_{pe}a/v_{Te}$ with ν/ω_{pe} as parameter, and these should be compared with those in Fig.3.

Fig.20 shows k_i/k_r versus $(v_\varphi/v_{Te})^2$ for $\omega_{pe}a/v_{Te} = 10$ with ν/ω_{pe} as parameter and should be compared with Fig.4. It clearly shows that for low phase velocities the attenuation is almost entirely due to Landau damping, but that for higher phase velocities even a small rate of collision leads to a damping which considerably exceeds the extremely weak

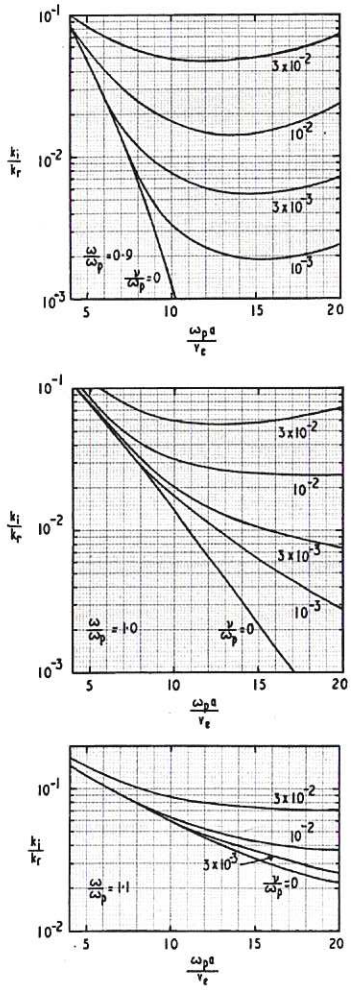

Fig.19
k_i/k_r versus $\omega_{pe}a/v_{Te}$ with ν/ω_{pe} as parameter for different values of ω/ω_{pe}

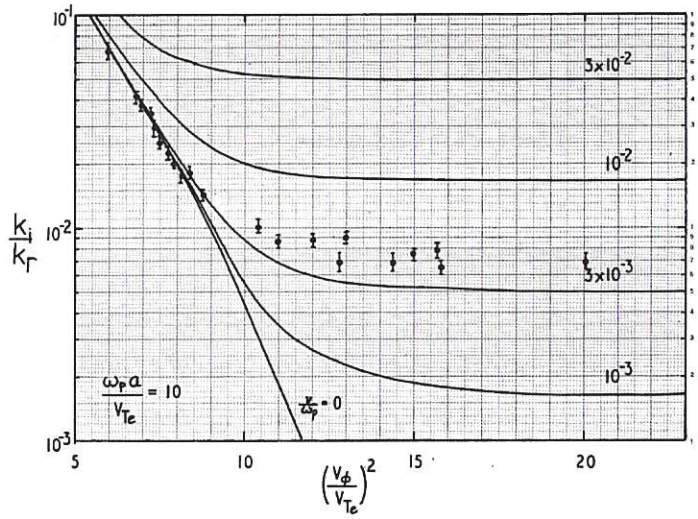

Fig.20
k_i/k_r versus $(v_\varphi/v_{Te})^2$ with ν/ω_{pe} as parameter and $\omega_{pe}a/v_{Te} = 10$

Landau damping. The experimental points, taken from Fig.17, show that if the damping of waves with phase velocities $\geq 3\, v_{Te}$ is due to electron-neutral atom collisions then $\nu/\omega_{pe} \sim 5\times 10^{-3}$, i.e. $\nu \sim 10^6\ s^{-1}$. The neutral gas pressure in the plasma vessel is 10^{-6} torr and although its composition is unknown is believed to consist mainly of sodium vapour and argon (this latter is used when it is necessary to bring the vessel to atmospheric pressure), but other permanent gases may be present. Even if all the gas was argon the collision rate for 0.2 eV electrons is $\leq 10^3\ s^{-1}$ (the mean free path λ_{ea} for 0.2 eV electrons in argon at 0°C and 1 torr ~ 1 mm [von Engel 1965, p.33]), and thus cannot account for the damping. If the damping arises from collisions with sodium atoms then its vapour pressure would need to be $\sim 10^{-6}$ torr (λ_{ea} for 0.2 eV electrons in sodium vapour at 1 torr and 0°C is $\sim 7\times 10^{-3}$ mm [Perel, Englander and Bederson 1962]). The saturated vapour pressure of sodium at 15°C, the temperature of the wall, is 10^{-9} torr but because of the presence of the hot plate, at a temperature ~ 2500 K, the pressure may be significantly higher in some parts of the vessel since the system is clearly not in thermal equilibrium. Experimentally ν/ω_{pe} increases with plasma density. For our experimental conditions ω_{pe} varies essentially as the square root of the neutral flux on to the hot plate [Hashmi, van der Houven van Oordt and Wegrowe 1970], whereas ν might be expected to vary linearly, thus giving some support to the view that the damping arises from electron-sodium atom collisions.

PART IV

NON-LINEAR EFFECTS

Linear plasma theory is based on the assumptions that any arbitrary perturbation in plasma can be Fourier analyzed into a linear superposition of wave modes, each mode having a development independent of any other, and that the waves do not modify the distribution function by particle trapping. For small amplitude waves these assumptions are well satisfied, but at larger amplitudes either or both can be violated.

Resonant mode coupling or parametric decay results in the simultaneous growth of other propagating plasma waves and a damping of the initial wave which exceeds its Landau value. Experimentally processes of this sort are easily recognized by examining the plasma fluctuation spectrum since they satisfy selection rules which, for three wave coupling, are

$$\omega_o = \omega_1 + \omega_2 \qquad \ldots (25)$$

$$\underline{k}_o = \underline{k}_1 + \underline{k}_2 \qquad \ldots (26)$$

where $(\omega_o, \underline{k}_o)$ is the large electron plasma wave and $(\omega_1, \underline{k}_1)$ and $(\omega_2, \underline{k}_2)$ are the decay products, and are characterized by a threshold [Dysthe and Franklin 1969]. Decay processes are the most important non-linearity for electron plasma waves whose phase velocities exceed $\sim 4\, v_{Te}$ where the Landau damping is weak, and have been identified for decay into another electron plasma wave and an ion wave [Franklin, Hamberger, Lampis and Smith 1971a] and for decay into higher order electron plasma wave modes [Franklin, Smith, Hamberger and Lampis 1971b].

Electrons which have velocities v in the range $v = v_\varphi \pm 2\sqrt{2\, e\varphi/m}$, where φ is the wave amplitude can become trapped in the wave potential wells where they oscillate with a characteristic 'bounce' frequency $\omega_B = k_o \left(\frac{e\varphi}{m}\right)^{\frac{1}{2}} = 2\pi/\tau_B$, or 'bounce' length $\lambda_B = \tau_B\, v_\varphi$, as discussed by Spitzer (1962). This can lead to a non-exponential damping of the wave with an instantaneous damping rate which is less than the linear Landau rate $\gamma_L = 2\pi/\tau_L$, or even to wave regrowth. If sufficient electrons are trapped for the equilibrium to become unstable other waves in the system can grow and the instantaneous damping rate exceeds γ_L [Franklin, Hamberger, Ikezi, Lampis and Smith 1972]. Both these non-linear effects have been observed [Franklin, Hamberger and Smith 1972] and an example of the reduction in local damping with increasing initial amplitude is shown in Fig.13. Whether measurements show linear or non-linear behaviour depends on the relative ordering of τ_B, τ_L and the observation time τ (or the corresponding lengths in spatial experiments). If $\tau_L \ll \tau_B$ then the behaviour is essentially linear; conversely if $\tau_L \gg \tau_B$ and $\tau \geq \tau_B$ then it is non-linear.

The trapped electron instability is readily identified and distinguished from decay instabilities because the frequencies of the growing side-band waves (ω,k), which may be above and below that of the large wave even in stationary plasma, depend on the wave amplitude (those of decay products do not) and do not satisfy the selection rules (25) and (26) but are approximately given by [Mima and Nishikawa 1971]

$$\omega - kv_\varphi \approx \pm \sqrt{2N+1}\,\omega_B . \qquad \ldots (27)$$

Trapped electron effects are the principal non-linearity for waves whose phase velocities $v_\varphi \leq 4\, v_{Te}$.

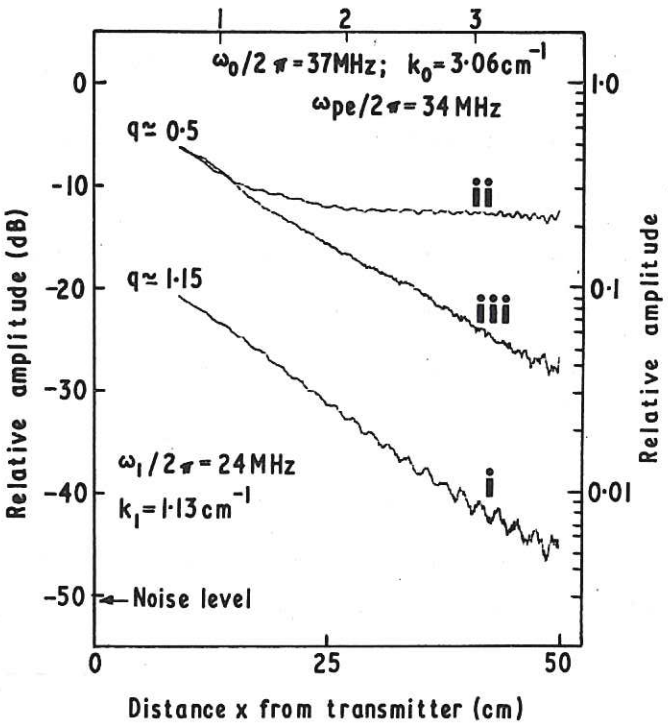

Fig.21
Raw experimental data showing relative spatial amplitude of (i) wave (ω_o, k_o) with initial amplitude $\varphi_o = 0.4$ mV; (ii) same wave but $\varphi_o \simeq 2.2$ mV; and (iii) same wave as (ii) but in presence of undamped wave (ω_1, k_1), launched at x = 67 cm with amplitude $\simeq 4$ mV and propagating in opposite direction to (ω_o, k_o). $k_i/k_o = 2.4 \times 10^{-2}$. $\Delta f = 0.3$ kHz, $n_e = 1.44 \times 10^7\ cm^{-3}$, $T_e = 2500$ K, $q = \gamma_L/\omega_B$

A demonstration that trapped electrons are responsible for the observed non-linear behaviour can be made by exciting a second electron plasma wave (ω_1, k_1) whose amplitude is comparable to that of the first but with different phase velocity, so that the only time invariant potential well has a phase velocity $(\omega_o - \omega_1)/(k_o - k_1)$ which is well removed from v_φ [Ott and Dum 1971]. For such conditions the non-exponential behaviour disappears and linear behaviour is recovered as shown in Fig.21.

ACKNOWLEDGEMENT

It is a pleasure to thank Mr W.J. McKay for his valuable technical assistance and the Science Research Council and United Kingdom Atomic Energy Authority for financial support.

REFERENCES

ANDERSEN, S.A., JENSEN, V.O., MICHELSEN, P. and NIELSEN, P., 1971, Phys. Fluids, 14, 728.

BARRETT, P.J., JONES, H.G. and FRANKLIN, R.N., 1968, Plasma Phys., 10, 911.

BHATNAGER, P.L., GROSS, E.P. and KROOK, M., 1954, Phys. Rev., 94, 511.

BOHM, D. and GROSS, E.P., 1949, Phys. Rev., 75, 1851.

BURT, J., LITTLE, P.F. and STOTT, P.E., 1969, Culham Laboratory Report CLM-R 98; Plasma Phys., 11, 789.

BUZZI, J.M., DOUCET, H.J. and GRESILLON, D., 1969, In Proc. 2nd Int. Conf. on Quiescent Plasmas, Paris, p.149.

BUZZI, J.M., DOUCET, H.J. and GRESILLON, D., 1970, Phys. Fluids, 13, 3041.

CHEN, F.F., ETIEVANT, C. and MOSHER, D., 1968, Phys. Fluids, 11, 811.

CLEMMOW, P.C. and DOUGHERTY, J.P., 1969, 'Electrodynamics of Particles and Plasmas'. Addison-Wesley.

DERFLER, H. and SIMONEN, T.C., 1966, Phys. Rev. Lett., 17, 172.

DYSTHE, K.B. and FRANKLIN, R.N., 1970, Plasma Phys., 12, 705.

von ENGEL, A.H., 1965, 'Ionized Gases'. Clarendon Press, Oxford University.

FRANKLIN, R.N., 1968, Plasma Phys., 10, 805.

FRANKLIN, R.N., HAMBERGER, S.M., IKEZI, H., LAMPIS, G. and SMITH, G.J., 1972, Phys. Rev. Lett., 28, 1114.

FRANKLIN, R.N., HAMBERGER, S.M., LAMPIS, G. and SMITH, G.J., 1971(a), Phys. Rev. Lett., 27, 1119.

FRANKLIN, R.N., HAMBERGER, S.M. and SMITH, G.J., 1972, Phys. Rev. Lett., 29, 914.

FRANKLIN, R.N., HAMBERGER, S.M. and SMITH, G.J., 1973, Plasma Phys., 15, 935.

FRANKLIN, R.N., SMITH, G.J., HAMBERGER, S.M. and LAMPIS, G., 1971(b), Phys. Lett., 36A, 473.

FRIED, B.D. and CONTE, S.D., 1961, 'The Plasma Dispersion Function'. Academic Press.

GENTLE, K.W., 1970, In 'Methods of Experimental Physics - Plasma Physics', 9A, (ed. Marton, L.). Academic Press.

GOULD, R.W., 1964, 'Propagation of Electrostatic Waves along a Plasma Column'. Unpublished.

HASHMI, M., van der HOUVEN van OORDT, A.J. and WEGROWE, J.-G., 1970, Nuclear Fusion, 10, 163.

KRALL, N.A. and TRIVELPIECE, A.W., 1973, 'Principles of Plasma Physics'. McGraw-Hill.

LANDAU, L.D., 1946, J. Phys. USSR, 10, 25.

LEE, A. and SCHMIDT, G., 1970, Phys. Fluids, 13, 2546.

MALMBERG, J.H. and WHARTON, C.B., 1966, Phys. Rev. Lett., 17, 175.

MALMBERG, J.H., WHARTON, C.B. and DRUMMOND, W.E., 1965, In Proc. Int. Conf. on Plasma Physics and Controlled Nuclear Fusion, Culham. Paper CN-21/116, p.485, vol.1, IAEA Vienna.

McKAY, D.H., 1967, D. Phil. Thesis, Oxford University.

MIMA, K. and NISHIKAWA, K., 1971, J. Phys. Soc. Japan, 30, 1722.

MONTGOMERY, D.C. and TIDMAN, D.A., 1964, 'Plasma Kinetic Theory'. McGraw-Hill.

OTT, E. and DUM, C.T., 1971, Phys. Fluids, 14, 959.

OTT, W., 1967, Z. Naturforschg., 22a, 1057.

PEREL, J., ENGLANDER, P. and BEDERSON, B., 1962, Phys. Rev., 128, 1148.

ROBINSON, F.N.H., 1962, 'Noise in Electrical Circuits'. Clarendon Press, Oxford University.

SILIN, V.P., 1960, Zh. Eksp. Teor. Fiz., 38, 1771, [English Translation: Sov. Phys. JETP, 11, 1277, (1960)].

SNEDDON, I.N., 1961, 'Special Functions of Mathematical Phyiscs and Chemistry'. Oliver and Boyd.

SPITZER, L., 1962, 'Physics of Fully Ionized Gases'. Interscience, John Wiley.

STIX, T.H., 1962, 'The Theory of Plasma Waves'. McGraw-Hill.

TROPMANN, M., 1970, Z. Naturforschg, 25a, 504.

APPENDIX 1

LINEAR HIGH FREQUENCY PERMITTIVITY OF PLASMA WITH A ONE-DIMENSIONAL ELECTRON VELOCITY DISTRIBUTION

In strongly magnetized, collisionless plasma the electron distribution function must satisfy the one-dimensional Vlasov equation

$$\frac{\partial f}{\partial t} + v \frac{\partial f}{\partial x} + \frac{eE}{m} \frac{\partial f}{\partial v} = 0 \qquad \ldots (A1.1)$$

which, because of the interaction between the particle distribution function and the electric field is inherently non-linear, and Poisson's equation

$$\frac{\partial E}{\partial x} = 4\pi e \int_{-\infty}^{+\infty} f_1(v)\, dv \ , \qquad \ldots (A1.2)$$

where the symbols have their usual meanings.

To linearize these equations suppose that the propagating electrostatic plasma wave, whose electric field varies like

$$E = E_o \exp i(\omega t - kx) \ , \qquad \ldots (A1.3)$$

causes a small perturbation to the equilibrium distribution function $f_o(v)$ so that the new distribution function $f(x,v,t)$ may be written

$$f(x,v,t) = f_o(v) + f_1(x,v,t) \qquad \ldots (A1.4)$$

Substituting this into (A1.1) we obtain

$$\frac{\partial f_1}{\partial t} + v \frac{\partial f_1}{\partial x} = - \frac{e}{m} E_o \exp i(\omega t - kx) \frac{\partial f_o}{\partial v}$$

which has a solution

$$f_1 = \frac{e}{m} i \frac{E_o \exp i(\omega t - kx)}{(\omega - kv)} \frac{\partial f_o}{\partial v} \qquad \ldots (A1.5)$$

Putting (A1.5) into (A1.2) and rearranging leads to

$$\left[1 + \frac{\omega_{pe}^2}{nk} \int_{-\infty}^{+\infty} \frac{\partial f_o / \partial v}{(\omega - kv)} dv \right] E_o \exp i(\omega t - kx) = 0 \qquad \ldots (A1.6)$$

which may be written

$$\epsilon(\omega,k)\, E(\omega,k) = 0 \ ,$$

and which has non-trivial solutions only when

$$\epsilon(\omega,k) = 0 \ . \qquad \ldots (A1.7)$$

This is the linearized solution to Vlasov's equation and $\epsilon(\omega,k)$ is the linear high frequency permittivity of unmagnetized plasma.

Because the plasma is strongly magnetized and we are interested here only in waves which propagate parallel to it, i.e. along the plasma column, we need consider only one-

dimensional velocity distributions for the unperturbed electrons, which we assume to be a one-dimensional Maxwellian :

$$f_o(v) = n\left(\frac{m}{2\pi\kappa T_e}\right)^{\frac{1}{2}} \exp\left(-\frac{1}{2}\,\frac{mv^2}{\kappa T_e}\right) = \frac{n}{\sqrt{\pi}\,v_{Te}} \exp\left(-\frac{v^2}{v_{Te}^2}\right). \qquad \ldots (A1.8)$$

The substitution of this into (A1.8) yields

$$\epsilon(\omega,k) = 1 - \frac{\omega_{pe}^2}{k^2 v_{Te}^2}\,\frac{2}{\sqrt{\pi}} \int_{-\infty}^{+\infty} \frac{x \exp(-x^2)}{\left(\frac{\omega}{kv_{Te}} - x\right)}\,dx \qquad \ldots (A1.9)$$

where $x = v/v_{Te}$.

We can write this in terms of The Plasma Dispersion Function [Fried and Conte 1961], defined by

$$Z(\zeta) = \frac{1}{\sqrt{\pi}} \int_{-\infty}^{+\infty} \frac{\exp(-x^2)}{x - \zeta}\,dx \qquad \ldots (A1.10)$$

where $\zeta = a + ib$ is a complex variable, and its derivative

$$Z'(\zeta) = \frac{2}{\sqrt{\pi}} \int_{-\infty}^{+\infty} \frac{x \exp(-x^2)}{\zeta - x}\,dx\ , \qquad \ldots (A1.11)$$

and obtain

$$\epsilon(\omega,k) = 1 - \frac{\omega_{pe}^2}{k^2 v_{Te}^2}\,Z'\left(\frac{\omega}{kv_{Te}}\right) . \qquad \ldots (A1.12)$$

This is the component of the high frequency plasma permittivity parallel to a strong magnetic field.

Both $Z(\zeta)$ and $Z'(\zeta)$ are complex, even when ζ is real, and have been tabulated for a wide range of complex ζ values by Fried and Conte (1961). Approximate expressions for $Z(\zeta)$ obtained by expansion of the function, are

$$Z(\zeta) = i\sqrt{\pi}\,\exp(-\zeta^2) - 2\zeta\left(1 - \frac{2}{3}\zeta^2 + \frac{4}{15}\zeta^4 - \frac{8}{105}\zeta^6 + \ldots\right) \qquad \text{for } \zeta \ll 1 \qquad \ldots (A1.13)$$

and

$$Z(\zeta) = i\sigma\sqrt{\pi}\,\exp(-\zeta^2) - \frac{1}{\zeta}\left(1 + \frac{1}{2\zeta^2} + \frac{3}{4\zeta^4} + \ldots\right) \qquad \text{for } \zeta \gg 1\ , \qquad \ldots (A1.14)$$

where σ is 0, 1 or 2 according to whether the imaginary part of ζ is <0, 0 or >0 respectively. Corresponding expressions for $Z'(\zeta)$ are readily obtained.

APPENDIX 2

COMPUTER PROGRAM TO SOLVE THE DISPERSION RELATION FOR ELECTRON PLASMA WAVES PROPAGATING IN A CYLINDRICAL PLASMA COLUMN

The program reproduced below is written in the form of a sequence of procedures which are called up in the main program. These procedures include ones for calculating the plasma dispersion function $Z(\zeta)$ as described by Franklin (1968) and Bessel functions of complex argument as developed by McKay (1967). Data for the program are in the sequence $U = \omega_{pe}a/v_{Te}$, $NU = \nu/\omega_{pe}$ (where ν is the electron collision frequency which, to solve (15) is put equal to zero), ACC = accuracy of iteration, N = limit to number of iterations, n = number of values of ω/ω_{pe} to follow for the fixed value of $\omega_{pe}a/v_{Te}$; then follows a sequence of three variables ω/ω_{pe}, approximate value of $k_r a$, approximate value of $k_i a$. The print-out gives the values of U, NU and ACC followed by a table of values in the order ω/ω_{pe}, $k_r a$, $k_i a$, k_i/k_r, $k_r\lambda_D$, $k_i\lambda_D$, $\omega^2/k^2 v_{Te}^2$, number of iterations.

The accuracy of the initial estimate for $k_r a$ becomes important at large values of ω/ω_{pe} if convergence on to a more heavily damped mode with a larger value of $k_r a$ is to be avoided. The roots are found by a two dimensional Newton's method and the program takes as the first two points $(k_r a, k_i a)$ and $(1.1\, k_r a,\ 1.1\, k_i a)$; it is therefore best to underestimate $k_r a$ and $k_i a$ by $\sim 10\%$.

```
'BEGIN' [                                    ]
'REAL' 'PROCEDURE' MODC(A,B); 'VALUE' A,B; 'REAL' A,B;
'IF' A =0 'AND' B=0 'THEN' MODC:=0 'ELSE'
'BEGIN' A:=ABS(A);B:=ABS(B); 'IF' A'GT'B 'THEN' MODC:= A/ COS(ARCTAN(B/
                        A))
        'ELSE' MODC:=B/COS(ARCTAN(A/B))
'END';
'PROCEDURE' PLASMADIS(X,Y,RZ,IZ,RZDASH,IZDASH); 'VALUE' X,Y;
'REAL' X,Y,RZDASH,IZDASH,RZ,IZ;
'BEGIN' 'IF' Y*Y/4.0+X*X/20.25'LT'1.0 'THEN' 'GOTO' TCHEB;
CONTFRACT:      'BEGIN' 'REAL' REB,IMB,RAA,IAA,RAB,IAB,RAC,IAC,RBA,IBA,
                        RBB,IBB,
                RBC,IBC,A,DEN,S,C,D,R,CAPI; 'INTEGER' I;
                S:=1.0; 'IF' Y'NE'0.0 'THEN' 'BEGIN' S:=Y/ABS(Y); Y:=AB
                        S(Y); 'END';
        REB:=RBB:=Y*Y-X*X+0.5; IMB:=IBB:=-2.0*X*Y; RAB:=X; IAB:=Y; RBC:
                        =1.0;
        IBC:=RAC:=IAC:=0.0;
        'FOR' I:=1 'STEP' 1 'UNTIL' 7 'DO' 'BEGIN' A:=-I*(I-0.5); REB:=
                        REB+2.0;
                RAA:=REB*RAB-IMB*IAB+A*RAC;
                IAA:=IMB*RAB+REB*IAB+A*IAC;
                RBA:=REB*RBB-IMB*IBB+A*RBC;
                IBA:=IMB*RBB+REB*IBB+A*IBC;
                RAC:=RAB; RAB:=RAA; IAC:=IAB; IAB:=IAA;
                RBC:=RBB; RBB:=RBA; IBC:=IBB; IBB:=IBA;
NORMALIZE;
'IF' ABS(RBA)'GT'1.0@15 'OR' ABS(IBA)'GT'1.0@15 'THEN' 'BEGIN' RA
                        B:=RAB*1.0@-15;
IAB:=IAB*1.0@-15; RAC:=RAC*1.0@-15; IAC:=IAC*1.0@-15;
RBB:=RBB*1.0@-15; IBB:=IBB*1.0@-15; RBC:=RBC*1.0@-15; IBC:=IBC
                        *1.0@-15 'END';
'END';
DEN:=RBA*RBA+IBA*IBA; RZ:=(RAA*RBA+IAA*IBA)/DEN; IZ:=(IAA*RBA-RAA*IBA)/
                        DEN;
NEGY;


'IF' S'LT'0.0 'THEN' 'BEGIN' C:=Y*Y-X*X; D:=2.0*X*Y; R:=-3.544907702*EX
                        P(C)*SIN(D);
        CAPI:=3.544907702*EXP(C)*COS(D); RZ:=RZ+R; IZ:=-IZ+CAPI 'END';
RZDASH:=-2.0*(1.0+X*RZ-S*Y*IZ); IZDASH:=-2.0*(X*IZ+S*Y*RZ); 'END';
'GOTO' OVER;
TCHEB:  'BEGIN' 'REAL' C,D,E,X2,Y2,X4,Y4,X6,Y6,X8,Y8,Y10,X10,X12,Y12,
                X14,Y14,X16,Y16,X18,Y18,X20,Y20,X22,Y22,X24,Y24,X26,Y26
                        ,
                X28,Y28,X30,Y30,X32,Y32,DIV,RNUM,INUM,RDEN,IDEN,RFRACT,
                        IFRACT;
        X2:=X*X-Y*Y; Y2:=2.0*X*Y; C:=1.77453851*EXP(-X2); D:=C*COS(Y2)
                        ;
        E:=C*SIN(Y2); X4:=X2*X2-Y2*Y2; Y4:=2.0*X2*Y2; X6:=X4*X2-Y4*Y2;
        Y6:=X4*Y2+Y4*X2; X8:=X4*X4-Y4*Y4; Y8:=2.0*X4*Y4; X10:=X4*X6-Y4*
                        Y6;
        Y10:=Y4*X6+X4*Y6; X12:=X6*X6-Y6*Y6; Y12:=2.0*X6*Y6; X14:=X6*X8-
                        Y6*Y8;
        Y14:=X6*Y8+Y6*X8; X16:=X8*X8-Y8*Y8; Y16:=2.0*X8*Y8; X18:=X8*X10
                        -Y8*Y10;
        Y18:=X8*Y10+X10*Y8; Y20:=2.0*X10*Y10; X20:=X10*X10-Y10*Y10;
        X22:=X10*X12-Y10*Y12; Y22:=X10*Y12+Y10*X12; X24:=X12*X12-Y12*Y1
                        2;
        Y24:=2.0*X12*Y12; X26:=X12*X14-Y12*Y14; Y26:=X12*Y14+X14*Y12;
        X28:=X14*X14-Y14*Y14; Y28:=2.0*X14*Y14; X30:=X14*X16-Y14*Y16;
        Y30:=X14*Y16+X16*Y14; X32:=X16*X16-Y16*Y16; Y32:=2.0*X16*Y16;
RNUM:=  62881393528.8
        -9466016230.15*X2
        +3245491278.91*X4
        -239814626.520*X6
        +36675354.1481*X8
        -1648557.33719*X10
        +150362.921964*X12
        -4370.84798976*X14
        +262.828105844*X16
        -4.88722590720*X18
        +0.19875947520*X20
```

```
          -0,00215654400*X22
          +0,00005701248*X24
          -0,00000026880*X26
          +0,00000000384*X28;
RDEN:=  62681393528,8
          +32454912789,1*X2
          +8113728197,27*X4
          +1305657411,05*X6
          +151549520,926*X8
          +13471068,5268*X10
          +949883,037143*X12
          +54279,0306939*X14
          +2544,32956378*X16
          +98,3315773440*X18
          +3,12873200640*X20
          +0,08126576640*X22
          +0,00169303680*X24
          +0,00002741760*X26
          +0,00000032640*X28
          +0,00000000256*X30
          +0,00000000001*X32;
INUM:=  -9466016230,15*Y2
          +3245491278,91*Y4
          -239814626,520*Y6
          +36675354,1481*Y8
          -1648557,33719*Y10
          +150362,921964*Y12
          -4370,84798976*Y14
          +262,828105344*Y16
          -4,88722590720*Y18
          +0,19875947520*Y20
          -0,00215654400*Y22
          +0,00005701248*Y24
          -0,00000026880*Y26
          +0,00000000384*Y28;
IDEN:=  32454912789,1*Y2

          +8113728197,27*Y4
          +1305657411,05*Y6
          +151549520,926*Y8
          +13471068,5268*Y10
          +949883,037143*Y12
          +54279,0306939*Y14
          +2544,32956378*Y16
          +98,3315773440*Y18
          +3,12873200640*Y20
          +0,08126576640*Y22
          +0,00169303680*Y24
          +0,00002741760*Y26
          +0,00000032640*Y28
          +0,00000000256*Y30
          +0,00000000001*Y32;
DIV:=RDEN*RDEN+IDEN*IDEN; RFRACT:=(RNUM*RDEN+IDEN*INUM)/DIV;
IFRACT:=(INUM*RDEN-IDEN*RNUM)/DIV; RZ:=E-2,0*(X*RFRACT-Y*IFRACT);
IZ:=D-2,0*(Y*RFRACT+X*IFRACT); RZDASH:=-2,0-2,0*(X*RZ-Y*IZ);
IZDASH:=-2,0*(X*IZ+Y*RZ); 'END';
OVER; 'END';


'PROCEDURE' SQRTC(A,B,C,D);'VALUE' A,B; 'REAL' A,B,C,D;
'BEGIN' 'REAL' THETA; 'IF' A'GT'0 'THEN' 'BEGIN' THETA:=0; 'GOTO' SOL
                        'END';
        'IF' A'LT'0'AND' (B'GT'0'OR' B=0) 'THEN' 'BEGIN' THETA:=3,14159
                        26535 90;
        'GOTO' SOL 'END';
        'IF' A'LT'0'AND'B'LT'0 'THEN' 'BEGIN' THETA:=-3,14159 26535 90;
        'GOTO' SOL 'END';
        'IF' A=0'AND' B=0 'THEN' 'BEGIN' C:=D:=0;'GOTO' RETURN 'END';
        'IF' A=0 'AND' B'GT'0 'THEN' 'BEGIN' C:=D:=SQRT(B/2);
        'GOTO' RETURN'END';
        'IF' A=0'AND' B'LT'0 'THEN' 'BEGIN' C:= SQRT(-B/2); D:=-C;
        'GOTO' RETURN 'END';
```

```
        SOLID:= SQRT(MODC(A,B)); A:=(ARCTAN (B/A)*THETA)/2;
        C:=D*COS(A);D:=D*SIN(A);
RETURN; 'END'SQRTC;


'PROCEDURE' JZSM(X,Y,JR,JI,YR,YI);'VALUE'  X,Y;
'REAL'  X,Y,JR,JI,YR,YI;

'BEGIN'  'REAL'  XX,YY,F,G,FD,GD,A,H,FE,GE,FF,GF,FG,GG,LR,LI,K,WA,WB,TP
                        ,XA,YA;
                XA:=ABS(X); YA:=ABS(Y);
        XX:=X'**'2-Y'**'2;YY:=2,0*XA*YA;F:=G:=FD:=GD:=FE:=GE:=FF:=GF:=F
                        G:=GG:=
                                        0,0;
        'FOR'  A:=1,52776628966@-19,-1,98858655989@-15,
        8,87648950577@-12,-1,90128586963@-8,
        2,25848557175@-5,-1,59547049907@-2,
        6,90220568183    ,-1,82980577559@+3,
        2,89641429881@+5,-2,58121327065@+7,
        1,15859974056@+9,-2,09892577626@+10,
        8,73153122922@+10  'DO'
        'BEGIN'  H:=F*XX-G*YY+A;G:=F*YY+G*XX;F:=H  'END';
        'FOR'  A:=1,0@-24,1,352@-21,1,211392@-18,
        9,59422464@-16,7,01749002248-13,
        4,77189321523@-10,2,99848417307@-7,
        1,71790077853@-4,8,79565198610@-2,
        3,91147817736@+1,1,44930559835@+4,
        4,19056361579@+6,8,39570310499@+8,
        8,73153122922@+10  'DO'
        'BEGIN'  H:=FD*XX-GD*YY+A;GD:=FD*YY+GD*XX;FD:=H  'END';
        'FOR'  A:=-7,38042951083@-26,-9,97834069863@-23,
        -8,60602031949@-19,-9,86990464621@-16,
        -8,70826788907@-13,-6,68110615768@-10,
        -4,57994302253@-7,-2,80622998236@-4,

        -1,51678240761@-1,-7,05648613251@+1,
        -2,71713120912@+4,-8,12317037590@+6,
        -1,67604925845@+9,-1,78941344066@+11'DO'
        'BEGIN'  H:=FE*XX-GE*YY+A;GE:=FE*YY+GE*XX;FE:=H  'END';
        'FOR'  A:=-2,62206530322@-17,3,68551979078@-13,
        -1,61922565438@-9,3,26303968134@-6,
        -3,51359697230@-3,2,16649521904    ,
        -7,83579857410@+2,1,64621638910@+5,
        -1,92046321417@+7,1,13036927597@+9,
        -2,76135258252@+10,1,72497098990@+11'DO'

        'BEGIN'  H:=FF*XX-GF*YY+A;GF:=FF*YY+GF*XX;FF:=H  'END';
        'FOR'  A:=1,352@-21,1,211392@-18,
        9,59422464@-16,7,01749002248-13,
        4,77189321523@-10,2,99848417307@-7,
        1,71790077853@-4,8,79565198610@-2,
        3,91147817736@+1,1,44930559835@+4,
        4,19056361579@+6,8,39570310499@+8,
        8,73153122922@+10  'DO'
        'BEGIN'  H:=FG*XX-GG*YY+A;GG:=FG*YY+GG*XX;FG:=H  'END';
        H:=FD'**'2+GD'**'2;JR:=(F*FD+G*GD)/H;JI:=(G*FD-F*GD)/H;
        LR:=0,5*LN(X'**'2+Y'**'2);
        LI:='IF' YA'GT'XA 'THEN' 1,57079632679-ARCTAN(XA/YA)
                'ELSE'  ARCTAN(YA/XA);
        K:=FG'**'2+GG'**'2;TP:=0,6366197723676;

        WA:=(FE*FG+GE*GG)/K*TP*LR;WB:= -(FE*GG-GE*FG)/K+TP*LI;
        YR:=(FF*FD+GF*GD)/H*JR*WA-JI*WB;
        YI:=(GF*FD-FF*GD)/H+JR*WB+JI*WA;
        'IF' X'LT'0,0 'THEN' 'BEGIN' JI :=- JI; YR:=YR-2,0*JI; YI:=2,0*
                        JR-YI 'END';
        'IF' Y'LT' 0,0 'THEN' 'BEGIN' JI:= - JI;YI := - YI 'END' ;
'END';
```

```
'PROCEDURE' JUSM(X,Y,JR,JI,YR,YI);'VALUE' X,Y;
'REAL' X,Y,JR,JI,YR,YI;

'BEGIN' 'REAL' XX,YY,F,G,FD,GD,A,H,FE,GE,FF,GF,LR,LI,WA,WB,TP,XA,YA;
                XA:=ABS (X) ; YA:= ABS (Y);
        XX:=X'**'2-Y'**'2;YY:=2,0*XA*YA;F:=G:=FD:=GD:=FE:=GE:=FF:=GF:=0
                          ,0;

        'FOR' A:=
     1,138620446283-19, -1,19207574908-15,  4,58387658614-12,
    -8,986230377873 -9,  1,03130729849 -5, -7,39535454409 -3,
     3,402777934853 +0, -1,005032477273 +3,  1,862491994003 +5,
    -2,060245822363 +7,  1,242263352623 +9, -3,441430993923+10,
     2,946891789873+11
       'DO'
        'BEGIN' H:=F*XX-G*YY+A;G:=F*YY+G*XX;F:=H  'END';
        'FOR'  A:=
     6,000000000023-24,  4,608000000013-20,  1,107025920003-16,
     1,700391813123-13,  2,004033208333-10,  1,940195641403 -7,
     1,582277032863 -4,  1,089563768323 -1,  6,247619264603 +1,
     2,883476192513 +4,  1,015405799213 +7,  2,421837434143 +9,
     2,946891789873+11
     'DO'

        'BEGIN' H:=FD*XX-GD*YY+A;GD:=FD*YY+GD*XX;FD:=H  'END';
        'FOR'  A:=
    -4,007020080713-20, -1,256294249693-16, -2,245398023473-13,
    -2,933418568363-10, -3,066423119633 -7, -2,656636141823 -4,
    -1,922447099753 -1, -1,149195619193 +2, -5,507204553503 +4,
    -1,997689732043 +7, -4,898998709503 +9, -6,111426115363+11

        'DO'
        'BEGIN' H:=FE*XX-GE*YY+A;GE:=FE*YY+GE*XX;FE:=H  'END';
        'FOR'  A:=
    -1,735899933603-17,  2,030818708123-13, -7,924394725483-10,

     1,503689071923 -6, -1,608304486073 -3,  1,035687246013 +0,
    -4,108899353263 +2,  9,966888355263 +4, -1,423713456533 +7,
     1,108109312253 +9, -4,041152394903+10,  4,955908053813+11
        'DO'

        'BEGIN' H:=FF*XX-GF*YY+A;GF:=FF*YY+GF*XX;FF:=H  'END';
        H:=FD'**'2+GD'**'2;JR:=(F*FD+G*GD)/H;JI:=(G*FD-F*GD)/H;
        A:=XA*FF-YA*GF;  GF:=(YA*FF+XA*GF)/2,0;  FF:=A/2,0;
        A:=XA*JR-YA*JI;  JI:=(YA*JR+XA*JI)/2,0;  JR:=A/2,0;
LR:=0,5*LN(X'**'2+Y'**'2);
        LI:='IF' YA 'GT' XA 'THEN' 1,570796326793-ARCTAN(XA/YA)
                'ELSE'  ARCTAN(YA/XA);
        TP:=0,6366197723676;

        XX:=X'**'2+Y'**'2;

        WA:=(FE*FD+GE*GD)/H+TP*LR;WB:= -(FE*GD-GE*FD)/H+TP*LI;
        YR:=(FF*FD+GF*GD)/H+JR*WA-JI*WB-TP*XA/XX;
        YI:=(GF*FD-FF*GD)/H+JR*WB+JI*WA+TP*YA/XX;
        'IF' X'LT' 0,0 'THEN' 'BEGIN' JR := -JR; YR := -YR -2,0 *JI;
        YI:=YI+2,0*JR; 'END';
        'IF' Y'LT'0,0 'THEN' 'BEGIN'  JI := - JI; YI:=-YI; 'END';

'END';


'PROCEDURE' HZLG(X,Y,HAR,HAI,HBR,HBI); 'VALUE' X,Y; 'REAL' X,Y,HAR,HAI,
                        HBR,HBI;
'BEGIN' 'REAL' XA,YA,D,XD,YD,FA,FB,FD,GA,GB,GD,H,MD,UR,UI,VR,VI,A,B,R,
C,S,WA,WB,XN,YN;
XA:=ABS (X); YA:= ABS(Y);
D:=XA'**'2+YA'**'2; XN:=XA/D; YN:=-YA/D; XD:=XN'**'2-YN'**'2; YD:=2,0*X
                        N*YN;
FA:=FB:=FD:=GA:=GB:=GD:=0,0;  'FOR' A:=
```

```
    -1,59413104640@+10, -4,03500671317@+12, -4,50329009019@+13,
    -9,83265118610@+13, -6,82721381775@+13, -1,92953566362@+13,
    -2,57254501661@+12, -1,78057207699@+11, -6,82299510142@ +9,
    -1,51035763151@ +8, -1,98062080760@ +6, -1,55215735960@ +4,
    -7,19365054481@ +1, -1,89609341842@ -1, -2,58162616308@ -4,
    -1,38730085225@ -7
  'DO' 'BEGIN' H:=FA*XD-GA*YD+A; GA:=FA*YD+GA*XD; FA:=H 'END'; 'FOR' A
                    :=

     7,00252160000@ +7, -1,66324367360@+11, -3,52313022701@+12,
    -9,85920227137@+12, -7,64058195768@+12, -2,27430296946@+12,
    -3,11307204488@+11, -2,18459739110@+10, -8,43528956496@ +8,
    -1,87549370742@ +7, -2,46591866003@ +5, -1,93559292643@ +3,
    -8,97989588132@ +0, -2,36845572761@ -2, -3,22613854510@ -5,
    -1,73412606531@ -3
  'DO' 'BEGIN' H:=FB*XD-GB*YD+A; GB:=FB*YD+GB*XD; FB:=H 'END'; 'FOR' A
                    :=
    -3,55555555555@+10, -5,01551020403@+12, -4,89081755506@+13,
    -1,01876147690@+14, -6,94233642259@+13, -1,94602233829@+13,
    -2,58440697016@+12, -1,78521775062@+11, -6,33341070067@ +9,
    -1,51173400478@ +8, -1,93170456015@ +6, -1,55266114468@ +4,
    -7,19498097550@ +1, -1,89627479028@ -1, -2,58172370767@ -4,
    -1,38730085225@ -7
'DO'
'BEGIN' H:=FD*XD+GD*YD+A; GD:=FD*YD-GD*XD; FD:=H 'END';
MD:=FD'**'2+GD'**'2; UR:=(FA*FD+GA*GD)/MD;  UI:=(FD*GA-FA*GD)/MD;
VR:=(FB*FD+GB*GD)/MD;  VI:=(FD*GB-FB*GD)/MD;
R:=VR*XN-VI*YN;  VI:=VI*XN+VR*YN;  VR:=R;
R:=SQRT(D); A:=SQRT((XA+R)/2,0);
B:=YA/(2,0*A); S:=XA-0,7853981633974; C:=COS(S); S:=SIN(S);
WA:=C*(UR+VI)-S*(UI-VR); WB:=S*(UR+VI)+C*(UI-VR);
FA:=0,79788456080029/(A'**'2+B'**'2);
'IF' YA 'LT'70 'THEN' FB:=EXP(YA) 'ELSE' FB:=1;
HAR:=(A*WA+B*WB)*FA/FB; HAI:=(A*WB-B*WA)*FA/FB;
WA:=C*(UR-VI)+S*(UI+VR); WB:=S*(VI-UR)+C*(UI+VR);
HBR:=(A*WA+B*WB)*FA*FB; HBI:=(A*WB-B*WA)*FA*FB;

'IF' X'LT' 0,0 'THEN' 'BEGIN' HBR := HBR+ 2,0*HAR; HBI:= -HBI- 2,0*HAI;
 HAR:= -HAR; 'END';
'IF' Y  'LT' 0,0 'THEN' 'BEGIN' FD:=HAR; HAR:=HBR; HBR:=FD;
 FD:= HAI; HAI:= - HBI; HBI:=-FD
                                'END';
'END';



'PROCEDURE' HULG(X,Y,HAR,HAI,HBR,HBI); 'VALUE' X,Y; 'REAL' X,Y,HAR,HAI,
                    HBR,HBI;
'BEGIN' 'REAL' XA,YA,D,XD,YD,FA,FB,FD,GA,GB,GD,H,MD,UR,UI,VR,VI,A,B,R,
C,S,WA,WB,XN,YN;
XA:=ABS(X); YA:=ABS(Y);
D:=XA'**'2+YA'**'2; XN:=XA/D; YN:=-YA/D; XD:=XN'**'2-YN'**'2; YD:=2,0*X
                    N*YN;
FA:=FB:=FD:=GA:=GB:=GD:=0,0;  'FOR' A:=

     6,97684234240@+10,  5,70480712179@+12,  4,78758830900@+13,
     9,56222292613@+13,  6,46444253482@+13,  1,81647b929818+13,
     2,42497839334@+12,  1,68440229249@+11,  6,48062517355@ +9,
     1,44018896014@ +8,  1,89536419915@ +6,  1,49009594322@ +4,
     6,92561289312@ +1,  1,83003126507@ -1,  2,49723460079@ -4,
     1,34461467219@ -7
  'DO' 'BEGIN' H:=FA*XD-GA*YD+A; GA:=FA*YD+GA*XD; FA:=H 'END'; 'FOR' A
                    :=
    -1,14737152000@ +9, -7,93489782336@+11, -1,19354012525@+13,
    -2,98279195729@+13, -2,21685459801@+13, -6,50373006544@+12,
    -8,86669886224@+11, -6,22620439000@+10, -2,40976662559@ +9,
    -5,37344879023@ +7, -7,08602559458@ +5, -5,57777810811@ +3,
    -2,59443280476@ +1, -6,85896387574@ -2, -9,36266010254@ -5,
    -5,04230502070@ -8
  'DO' 'BEGIN' H:=FB*XD-GB*YD+A; GB:=FB*YD+GB*XD; FB:=H 'END'; 'FOR' A
                    :=
     2,13333333333@+10,  3,90095238095@+12,  4,13838408504@+13,
     8,98907185503@+13,  6,28116152520@+13,  1,79034055123@+13,
```

```
     2,406172036708+12,  1,677022735468+11,  6,464037149528 +9,
     1,437990882618 +8,  1,893628501948 +6,  1,469287220428 +4,
     6,923472259508 +1,  1,829738832748 -1,  2,497077028758 -4,
     1,344614672198 -7
   'DO'
'BEGIN' H:=FD*XD-GD*YD+A; GD:=FD*YD+GD*XD; FD:=H 'END';
MD:=FD'**'2+GD'**'2; UR:=(FA*FD+GA*GD)/MD;  UI:=(FD*GA-FA*GD)/MD;
VR:=(FB*FD+GB*GD)/MD;  VI:=(FD*GB-FB*GD)/MD;
R:=VR*XN-VI*YN;  VI:=VI*XN+VR*YN;  VR:=R;
R:=SQRT(D); A:=SQRT((XA+R)/2,0);
B:=YA/(2,0*A); S:=XA-2,356194490191; C:=COS(S); S:=SIN(S);
WA:=C*(UR+VI)-S*(UI-VR); WB:=S*(UR+VI)+C*(UI-VR);
FA:=0,7978845608029/(A'**'2+B'**'2);
'IF' YA'LT'70 'THEN' FB:=EXP(YA) 'ELSE' FB:=1;
HAR:=(A*WA+B*WB)*FA/FB; HAI:=(A*WB-B*WA)*FA/FB;
WA:=C*(UR-VI)+S*(UI+VR); WB:=S*(VI-UR)+C*(UI+VR);
HBR:=(A*WA+B*WB)*FA*FB; HBI:=(A*WB-B*WA)*FA*FB;
'IF' X'LT'0,0 'THEN' 'BEGIN' HAI:= - HAI; HBR:= - HBR - 2,0*HAR;
 HBI:=  HBI-2,0*HAI; 'END';
'IF' Y'LT'0,0 'THEN' 'BEGIN' FD:=HAR; HAR:=HBR; HBR:= FD; FD:=HAI;
HAI:= - HBI; HBI:=-FD
                                    'END';

'END';



'PROCEDURE' BESC(M,X,Y,U,V); 'VALUE' M,X,Y; 'INTEGER' M; 'REAL' X,Y,U,V
                            ;
'BEGIN' 'REAL' A,B;
'IF' MODC(X,Y)'LT'9 'THEN'
'BEGIN' 'IF' M'NE'0 'THEN'
        'BEGIN' JUSM(X,Y,U,V,A,B); U:=M*U;V:=M*V; 'END'
        'ELSE' JZSM(X,Y,U,V,A,B);
'END'

'ELSE' 'IF' M=0 'THEN' 'BEGIN' HZLG(X,Y,U,V,A,B);
        'IF' ABS(Y)'LT'70 'THEN' 'BEGIN' U:=(U+A)/2; V:=(V+B)/2 'END'
        'ELSE' 'IF' Y'GT'69 'THEN' 'BEGIN' U:= A/2; V:=B/2 'END'
         'ELSE' 'BEGIN' U:=U/2;
        V:=V/2 'END'
        'END'
'ELSE' 'BEGIN' HULG(X,Y,U,V,A,B);
        'IF' ABS(Y)'LT'70 'THEN' 'BEGIN' U:=M*(U+A)/2; V:=M*(V+B)/2;
                                'END'
        'ELSE' 'IF' Y'GT'69 'THEN' 'BEGIN'  U:=M*A/2; V:=M*B/2 'END'
        'ELSE' 'BEGIN' U:=M*U/2; V:=M*V/2; 'END';
        'END'
'END';

'PROCEDURE' HANC(M,X,Y,U,V); 'VALUE' M,X,Y; 'INTEGER' M; 'REAL' X,Y,U,V
                            ;
'BEGIN' 'REAL' A,B;
'IF' MODC(X,Y)'LT'9'THEN'
'BEGIN' 'IF' M=0 'THEN' 'BEGIN' JZSM(X,Y,U,V,A,B); U:=U-B; V:=V+A;'END'
        'ELSE' 'BEGIN' JUSM(X,Y,U,V,A,B);U:=M*(U-B); V:=M*(V+A) 'END'
'END'
'ELSE' 'IF' M'NE'0 'THEN' 'BEGIN' HULG(X,Y,U,V,A,B);U:=M*U; V:=M*V;
                                'END'
'ELSE' HZLG(X,Y,U,V,A,B);
'END';


'PROCEDURE' F(W,U,NU,KRA,KIA,FR,FI); 'VALUE' W,U,NU,KRA,KIA;
'REAL' W,U,NU,KRA,KIA,FR,FI;
'BEGIN' 'REAL' ZR,ZI,K,RZ,IZ,RZDASH,IZDASH,A,B,C,D,E,G,AA,BB,ER,EI,RARG
                            ,IARG,RJO,IJO,
        RJI,IJI,RKO,IKO,RKI,IKI;
        K:=KRA*KRA+KIA*KIA; ZR:=W*U*(KRA+NU*KIA/W)/K; ZI:=W*U*(-KIA+NU*
                            KRA/W)/K;
        PLASMADIS(ZR,ZI,RZ,IZ,RZDASH,IZDASH);
        A:=-U*U/(K*K)*((KRA*KRA-KIA*KIA)*RZDASH+2,0*KRA*KIA*IZDASH);
```

```
        B:=U*U/(K*K)*(2,0*KRA*KIA*RZDASH-(KRA*KRA-KIA*KIA)*IZDASH);
        C:=1,0; D:=NU/W; E:=1,0+0,5*NU/W*IZDASH; G:=0,5*NU/W*RZDASH;
        ER:=((A*C-B*D)*E-G*(B*C+A*D))/(E*E+G*G); ER:=ER+1,0;
        EI:=((B*C+A*D)*E+G*(A*C-B*D))/(E*E+G*G);
        SQRTC(ER,EI,AA,BB); RARG:=-(BB*KRA+AA*KIA); IARG:=AA*KRA-BB*KI
                        A;
        BESC(0,RARG,IARG,RJO,IJO); BESC(1,RARG,IARG,RJI,IJI);
        HANC(0,-KIA,KRA,RKO,IKO); HANC(1,-KIA,KRA,RKI,IKI);
        FR:=RJO*RKI-IJO*IKI-AA*(RKO*RJI-IKO*IJI)+BB*(RKO*IJI+IKO*RJI);
        FI:=IJO*RKI+RJO*IKI-BB*(RKO*RJI-IKO*IJI)-AA*(RKO*IJI+IKO*RJI);
'END';


'PROCEDURE' DISPERSION(F,W,U,NU,KRA,KIA,ACC,KRACC,KIACC,N,M);
        'VALUE' W,U,NU,KRA,KIA,N,ACC; 'REAL' W,U,NU,KRA,KIA,ACC,KRACC,K
                        IACC;
        'INTEGER' N,M; 'PROCEDURE' F;
        'COMMENT'(XX1,XX2,XX3,XX4,XX5,XX6,XX7);
        'VALUE'XX1,XX2,XX3,XX4,XX5;
        'REAL'XX1,XX2,XX3,XX4,XX5,XX6,XX7;
'BEGIN' 'REAL' RF,IF,DELX,DELY,RF0,IF0,RF1,IF1,RF2,IF2,D01,D02,D12,DENO
                        M,MOD;
        M:=0; DELX:=0,1*KRA; DELY:=0,1*KIA;
LOOP:   M:=M+1; F(W,U,NU,KRA,KIA,RF0,IF0); F(W,U,NU,KRA+DELX,KIA,RF1,IF
                        1);
        F(W,U,NU,KRA,KIA+DELY,RF2,IF2); D01:=RF0*IF1-RF1*IF0;
        D02:=RF0*IF2-RF2*IF0; D12:=RF1*IF2-RF2*IF1; DENOM:=D12-D02+D01;
        KRACC:=KRA-DELX*D02/DENOM; KIACC:=KIA+DELY*D01/DENOM;
        MOD:=ABS(KRACC-KRA)+ABS(KIACC-KIA);
'IF' MOD'GT'ACC 'AND' M'LT'N 'THEN' 'BEGIN' DELX:=0,25*(KRACC-KRA); DEL
                        Y:=0,25*(KIACC
                    -KIA); KRA:=KRACC; KIA:=KIACC; 'GOTO' LOOP;
'END' 'END';


'REAL' W,U,NU,ACC,KRA,KIA,KRACC,KIACC; 'INTEGER' I,M,N,CAPN,F1,F2,F3;

F1:=FORMAT('('2S+D,DDDDDD@+ND')'); F2:=FORMAT('('2S+D,DDDDDD@+NDC
                        ')');
F3:=FORMAT('('-D,DDDDDD@+ND')');
        OPEN(220); OPEN(240);
START;  U:=READ(220);
        NU:=READ(220);
        ACC:=READ(220);
        CAPN:=READ(220);
        N:=READ(220);
        'IF' N=0 'THEN' 'GOTO' VER;
        WRITETEXT(240,'('''('4S')'WAONVE'('8S')'NUONW'('8S')
             'ACC'('C')''')');
        WRITE(240,F1,U);
        WRITE(240,F1,NU);
        WRITE(240,F2,ACC);
        WRITETEXT(240,'('''('5S')'W/WP'('11S')'KRA'('12S')'KIA'
             ('11S')'KI/KR'('11S')'KRL'('12S')'KIL'('12S')'
             WSQ/VTHSQ'('C')''')');
         'FOR' I:=1 'STEP' 1 'UNTIL' N 'DO' 'BEGIN'
             W:=READ(220);
             KRA:=READ(220);
             KIA:=READ(220);
             DISPERSION(F,W,U,NU,KRA,KIA,ACC,KRACC,KIACC,CAPN,M);
             WRITE(240,F3,W);
             WRITE(240,F1,KRACC);
             WRITE(240,F1,KIACC);
             WRITE(240,F1,KIACC/KRACC);
             WRITE(240,F1,KRACC/U);
             WRITE(240,F1,KIACC/U);
             WRITE(240,F1,(W*U/KRACC)'**'2);
             WRITE(240,FORMAT('('S-NDD')'),M);
             WRITETEXT(240,'('--ITERATIONS'('C')''')');
             'END';
         WRITETEXT(240,'('''('CCCC')''')'); 'GOTO' START;
VER:    CLOSE(220); CLOSE(240);
'END';
```

APPENDIX 3

CHANGE IN DAMPING RATE CAUSED BY A SMALL CHANGE IN PLASMA DENSITY

If there is an axial density gradient the phase velocity and therefore the damping length of a wave changes along the plasma column. Here we relate the change in the linear damping rate $\Delta\gamma_L$ to small changes in the plasma frequency $\Delta\omega_{pe}$ due to small variations in the plasma density.

The linear Landau damping rate γ_L of an electron plasma wave propagating in a Maxwellian plasma may by combining (1a) and (2a) be written

$$\gamma_L = \sqrt{\frac{\pi}{8}}\,\frac{\omega_{pe}}{k^3\lambda_D^3}\exp\left(-\frac{1}{2k^2\lambda_D^2}-\frac{3}{2}\right)$$

$$= \sqrt{\frac{\pi}{8}}\,\frac{\omega_{pe}}{\alpha^{\frac{3}{2}}}\left(\frac{3}{2}\right)^{\frac{3}{2}}\exp\left(-\frac{3}{4\alpha}-\frac{3}{2}\right), \qquad \ldots (A3.1)$$

where $\alpha = \frac{3}{2}k^2\lambda_D^2$.

Differentiating (A3.1) gives

$$\frac{1}{\gamma_L}\,\frac{d\gamma_L}{d\omega_{pe}} = \frac{1}{\omega_{pe}} - \frac{3}{2\alpha}\,\frac{d\alpha}{d\omega_{pe}} + \frac{3}{4\alpha^2}\,\frac{d\alpha}{d\omega_{pe}} \qquad \ldots (A3.2)$$

Using the approximate (Bohm and Gross) dispersion relation

$$\omega = \omega_{pe}\,(1+\alpha)$$

we obtain

$$\frac{d\alpha}{d\omega_{pe}} = -\frac{\omega}{\omega_{pe}^2},$$

and substituting this into (A3.2) yields

$$\frac{\Delta\gamma_L}{\gamma_L} = \frac{\Delta\omega_{pe}}{\omega_{pe}}\left[1+\frac{3}{2\alpha}\,\frac{\omega}{\omega_{pe}}\left(1-\frac{1}{2\alpha}\right)\right] \qquad \ldots (A3.3)$$

This relation is plotted in Fig.22 for several values of the parameter ω/ω_{pe} and clearly shows that a small change in ω_{pe} leads to a considerable change in γ_L. The upper parts of the graph are shown by dashed lines because the approximations used to obtain (A3.3) are no longer justified. A numerical example will serve to show the sensitivity of damping to number density variation. For $\omega/\omega_{pe} = 1.10$, a variation of 1.0% in number density causes a 33% variation in damping rate.

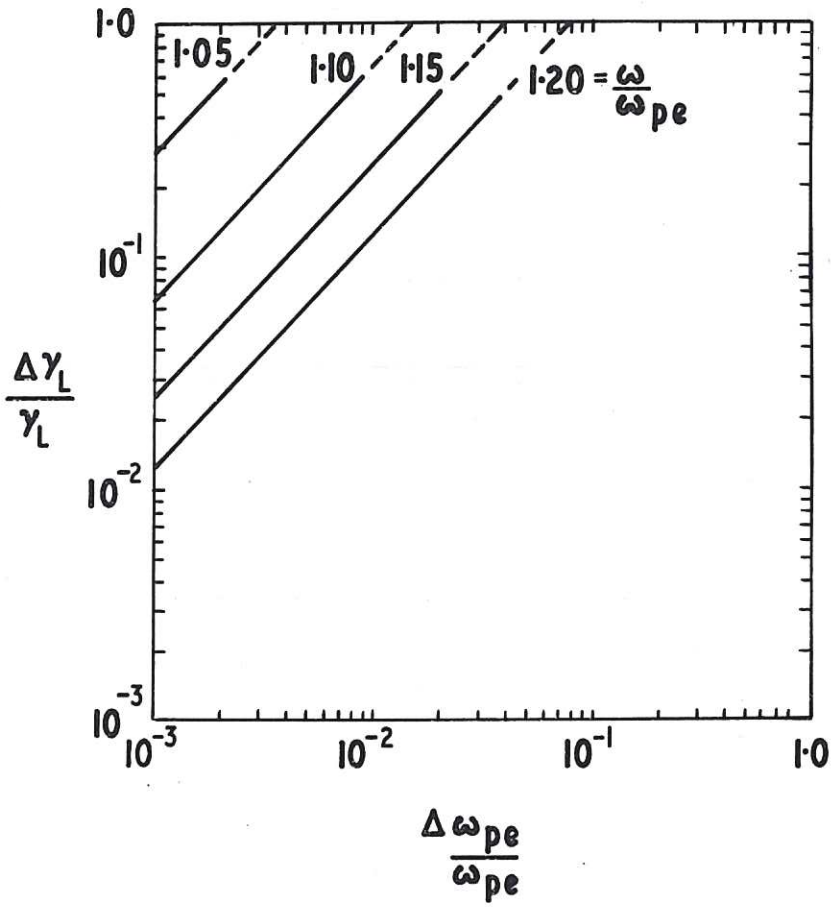

Fig.22
Fractional change in damping rate of electron plasma wave caused by a small change in plasma density (frequency)

APPENDIX 4

RELATION BETWEEN TEMPORAL AND SPATIAL DAMPING OF ELECTRON PLASMA WAVES

Quite generally we may write for propagating electrostatic waves

$$\epsilon(\Omega,K) = 0 \ . \qquad \ldots (A4.1)$$

For the initial value problem Ω is complex, K is real and thus

$$\epsilon(\omega + i\,\gamma_L\,, k_r) = 0 \ .$$

Expanding in a Taylor series

$$\mathrm{Re}\ \epsilon(\omega,k_r) + i\,\mathrm{Im}\,\epsilon(\omega,k_r) + i\,\gamma_L \frac{\partial}{\partial k}\epsilon(\omega,k_r) + \ldots = 0. \qquad \ldots (A4.2)$$

Alternatively, for Ω real and K complex (i.e. boundary value case)

$$\epsilon(\omega,k_r + ik_i) = 0 \ ,$$

and again expanding

$$\mathrm{Re}\ \epsilon(\omega,k_r) + i\,\mathrm{Im}\,\epsilon(\omega,k_r) + ik_i \frac{\partial}{\partial k}\epsilon(\omega,k_r) + \ldots = 0. \qquad \ldots (A4.3)$$

Ignoring second and higher order terms the roots of (A4.2) and (A4.3) are given by

$$\mathrm{Re}\ \epsilon(\omega,k_r) = 0 \qquad \text{in both cases,} \qquad \ldots (A4.4)$$

and by

$$\frac{\gamma_L}{\omega} = -\frac{\mathrm{Im}\ \epsilon(\omega,k_r)}{\omega \dfrac{\partial\epsilon}{\partial\omega}} \ , \qquad \ldots (A4.5)$$

$$\frac{k_i}{k_r} = -\frac{\mathrm{Im}\ \epsilon(\omega,k_r)}{k_r \dfrac{\partial\epsilon}{\partial k}} \qquad \ldots (A4.6)$$

for the temporal and spatial cases respectively. From these two last equations it is readily noted that

$$\gamma_L = k_i \ \frac{\partial\epsilon/\partial k}{\partial\epsilon/\partial\omega} \ . \qquad \ldots (A4.7)$$

Differentiating (A4.4)

$$\partial\epsilon(\omega,k_r) = \frac{\partial\epsilon}{\partial\omega}\,d\omega + \frac{\partial\epsilon}{\partial k}\,dk = 0$$

so that

$$\frac{\partial\epsilon/\partial k}{\partial\epsilon/\partial\omega} = -\ \frac{d\omega}{dk} = -\ v_{gr} \ . \qquad \ldots (A4.8)$$

Thus (A4.7) becomes

$$\gamma_L = -\ k_i \frac{d\omega}{dk} \ , \qquad \ldots (A4.9)$$

showing that γ_L and k_i are related by the wave group velocity.

For lightly damped waves ($k_i/k_r \ll 1$) this result has been proved rigorously by Lee and Schmidt (1970) in a treatment which explicitly retains the singular integral which describes Landau damping.

HER MAJESTY'S STATIONERY OFFICE

Government Bookshops

49 High Holborn, London WC1V 6HB
13a Castle Street, Edinburgh EH2 3AR
109 St Mary Street, Cardiff CF1 1JW
Brazennose Street, Manchester M60 8AS
50 Fairfax Street, Bristol BS1 3DE
258 Broad Street, Birmingham B1 2HE
80 Chichester Street, Belfast BT1 4JY

Government publications are also available through booksellers